

## Journal Pre-proof

Magnetic fabric of loess and its significance in Pleistocene environment reconstructions

Balázs Bradák, Yusuke Seto, Martin Chadima, József Kovács, Péter Tanos, Gábor Újvári, Masayuki Hyodo



PII: S0012-8252(20)30431-1

DOI: <https://doi.org/10.1016/j.earscirev.2020.103385>

Reference: EARTH 103385

To appear in: *Earth-Science Reviews*

Received date: 29 June 2020

Revised date: 24 September 2020

Accepted date: 24 September 2020

Please cite this article as: B. Bradák, Y. Seto, M. Chadima, et al., Magnetic fabric of loess and its significance in Pleistocene environment reconstructions, *Earth-Science Reviews* (2020), <https://doi.org/10.1016/j.earscirev.2020.103385>

This is a PDF file of an article that has undergone enhancements after acceptance, such as the addition of a cover page and metadata, and formatting for readability, but it is not yet the definitive version of record. This version will undergo additional copyediting, typesetting and review before it is published in its final form, but we are providing this version to give early visibility of the article. Please note that, during the production process, errors may be discovered which could affect the content, and all legal disclaimers that apply to the journal pertain.

© 2020 Published by Elsevier.

**Magnetic fabric of loess and its significance in Pleistocene environment reconstructions**

Balázs Bradák<sup>1\*</sup>, Yusuke Seto<sup>2</sup>, Martin Chadima<sup>3,4</sup>, József Kovács<sup>5</sup>, Péter Tanos<sup>6</sup>, Gábor Újvári<sup>7,8</sup>,  
Masayuki Hyodo<sup>2,9</sup>

<sup>1</sup>Dept. of Physics, Univ. of Burgos, Av. de Cantabria, s/n, Burgos, Spain, 09006

<sup>2</sup>Dept. of Planetology, Kobe Univ., Nada, Kobe, Japan, 657-8501

<sup>3</sup>AGICO, Inc. Jecna 29a Brno, Czech Republic, CZ62100

<sup>4</sup> Institute of Geology of the Czech Academy of Sciences, Prague, Czech Republic

<sup>5</sup>Dept. of Physical and Applied Geology, ELTE Eötvös Loránd Univ., 1/C, Pázmány P. st, Budapest,  
Hungary, H-1117

<sup>6</sup>Szent István Univ., 1 Práter Károly st. Gödöllő, Hungary, H-2100

<sup>7</sup>Dept. of Lithospheric Research, Univ. of Vienna 14 Althanstrasse, Vienna, Austria, A-1090

<sup>8</sup>Institute for Geological and Geochemical Research, Research Centre for Astronomy and Earth  
Sciences of the HAS, 45 Budaörsi st., Budapest, Hungary, H-1112.

<sup>9</sup>Research Center for Inland Seas, Kobe Univ., Nada, Kobe, Japan, 657-8501

\*Corresponding author: Balázs Bradák, bradak.b@gmail.com

**Abstract**

A summary of approximately three decades and greater than thirty loess magnetic fabric studies is presented here. The revised studies cover various loess regions from the Chinese Loess Plateau across the European Loess Belt to Alaska.

Although there is still an ongoing argument about the feasibility of the magnetic fabric of loess in paleowind reconstructions, the determination of prevailing wind direction during various periods of

the Pleistocene is the main goal of magnetic anisotropy analysis of the revised loess successions. The magnetic fabric analysis of loess from Chinese Loess Plateau provided significant information about the characteristics of paleomonsoon in East Asia, and the results from other loess regions, such as Alaska, the European Loess Belt, and Siberia, are also promising. As it is shown in this review, the synthesis of the paleowind direction results from the studied profiles may already provide a significant foundation for future climate models by the reconstruction of key climate centres and main continental level wind tracks.

Besides the reconstruction of prevailing paleowind directions, there are numerous loess magnetic fabric studies using magnetic anisotropy parameters in the reconstruction of the characteristics of long-term climate trends, climate transitions and glacial- interglacial cycles.

There are some lesser known aspects contributing to magnetic fabric of loess, such as the influence of various types of magnetic contributors on the overall fabric (i.e. the study of sub-fabrics) and their role in environment reconstruction. Besides the identification of aeolian magnetic fabric, not so many studies focus on the magnetic anisotropy characteristics of materials, possibly developed by water-lain sedimentation, pedogenesis, mass movements and permafrost activity.

Novel results from Hungarian loess, especially from Paks, connected to some of the latter topics are also presented. Such topics include the analysis of the nanofabric in paleosols, developed by pedogenesis, the comparison of magnetic fabric, formed during high energy transportation by aeolian or aquatic agents and the periodicity analysis of magnetic parameters during the early Middle Pleistocene. New research lines, introduced in this review, may inspire new researches, and provide new perspectives for the next generation of magnetic anisotropy studies of loess successions.

**Keywords:** loess and paleosol successions; magnetic fabric; Quaternary; paleoenvironment

Abbreviations<sup>1</sup>

---

<sup>1</sup> AMS-anisotropy of low-field magnetic susceptibility; APARM-anisotropy of partial remanence; AARM-anisotropy of total anhysteretic remanence;  $\beta$ -imbrication angle; CA-cluster analysis; Carp.-Carpathians; CIAM-Continental ice sheet air mass; CLP-Chinese Loess Plateau; cpo-crystallographic preferred (crystallographic axis) orientation; EASM-East Asian Summer Monsoon; EAWM-East Asian Winter Monsoon; EDS-Energy-dispersive X-ray spectroscopy; Hc-coercivity; Hcr-remnant coercive force; ELB-European Loess Belt; F-foliation; fdAMS-anisotropy of frequency-dependent magnetic susceptibility; IRM-isothermal remanent magnetization; ISM-Indian Summer Monsoon;  $\kappa$ lf-volumetric magnetic susceptibility;  $\kappa$ max-maximum principal susceptibility;  $\kappa$ int-intermediate principal susceptibility;  $\kappa$ min-minimum principal susceptibility;  $\kappa$ T-temperature variation in magnetic susceptibility;  $X_{lf}$ -mass magnetic susceptibility;  $X_{fd}$ -mass frequency dependent magnetic susceptibility;  $X_{fs}$ -normalized mass frequency dependent magnetic susceptibility; L-lineation; MD-multidomain; MFD- Mediterranean Front Depression; Mrs-saturation remanence; Ms-saturation magnetisation; opAMS-anisotropy of out-of-phase magnetic susceptibility; pdo-preferred dimensional orientation; Pj-corrected degree of anisotropy; PSD-pseudo-single domain; psd-power spectrum density; q-shape factor; (S)SD-(stable) single domain; SEM-scanning electron microscope; SH-Siberian High; SP-superparamagnetic; T-shape parameter; TH-Tibetan High; W-Westerlies; WSA-Wavelet spectrum analysis

## 1. Introduction

Numerous studies have assessed the magnetic fabric (MF) of geological and planetary materials, including sedimentary rocks. This short summary reviews the studies that play important roles in the interpretation of the magnetic fabric of loess and paleosols.

Anisotropy of low-field magnetic susceptibility (AMS) was reported as a useful tool to determine paleocurrent or paleodirection by Graham (1954). The application of magnetic anisotropy measurements has increased rapidly since Graham's pioneering study, and this technique is an essential method in a wide range of fields in Earth and planetary science (e.g., Hrouda, 1982; Tarling and Hrouda, 1993; Parés, 2015; Bilardello, 2016).

Following the study of Graham (1954), the first studies on the connection between depositional processes observed sedimentary structures and the magnetic fabric (e.g., Granar, 1958; Rees 1961). Such works and subsequent studies in the 1960s laid the foundation of magnetic anisotropy studies of sediments, i.e., the use of the magnetic fabric characteristics to determine the orientation of (paleo)currents responsible for sediment transportation (e.g., Rees, 1965) (Fig. 1).

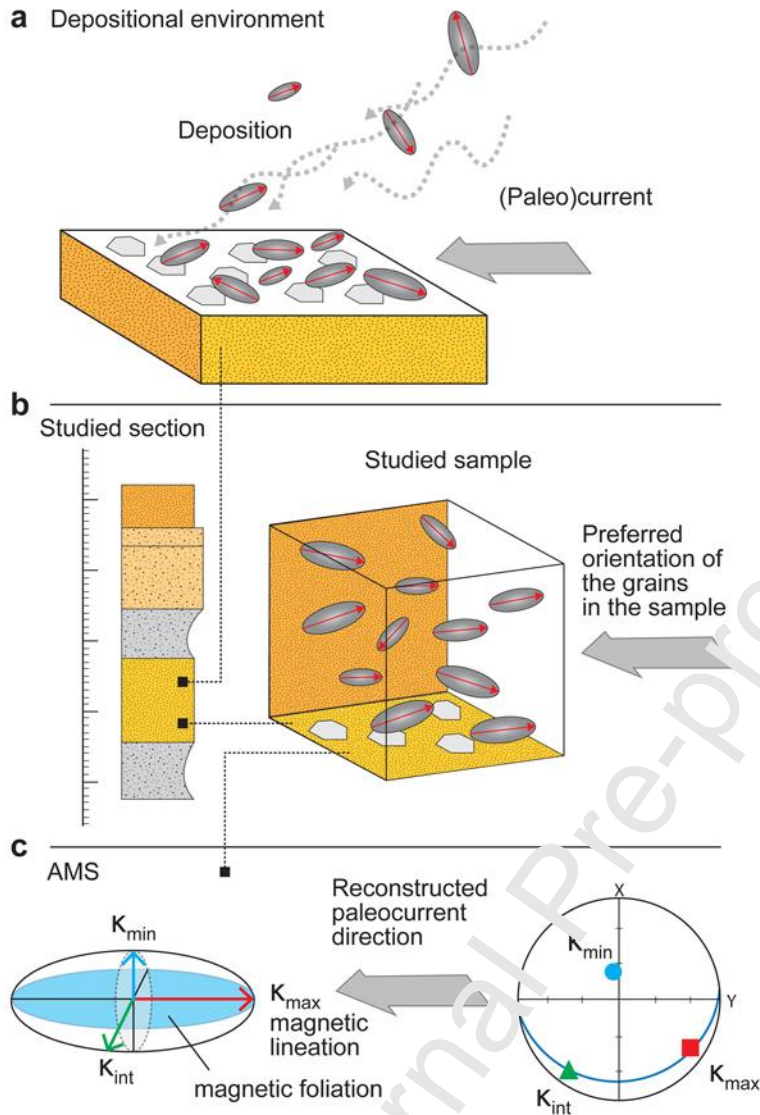


**Figure 1.** The connection between the depositional environment (a), the sedimentary fabric of rocks (b) and the magnetic fabric, defined from anisotropy of magnetic susceptibility (AMS) (c).  $K_{max}$ ,  $K_{int}$  and  $K_{min}$ , represent the principal susceptibility axes; the AMS ellipsoid serves as the geometrical visualization of the tensor and the stereonet represents the projection of the principal susceptibility directions (square, triangle, and circle) and magnetic foliation plane (great circle). More detailed information can be found in Section 3.2 and Tarling and Hrouda (1993).

As a part of the evaluation of the role of magnetic fabric analysis in the reconstruction of sedimentary environments, a series of studies was performed in a laboratory environment. Although such experiments mainly reconstructed depositional processes in an idealized and wet depositional

environment, these observations play fundamental role in the interpretation of the magnetic fabric of loess (Rees, 1966, 1968, 1983; Rees and Woodall, 1975; Ellwood and Howard, 1981). Such experimental studies present a collection of several fabric types, representing various sedimentary environments, and represent one of the most significant reference materials for the characterization of the fabric of natural sediments.

Along with the first reviews (e.g., Hrouda, 1982, Tarling and Hrouda, 1993), a few studies were performed to separate the magnetic fabric of sediments formed in different depositional environments (e.g., Taira 1989). The study separated the magnetic fabric related to various sedimentary structures (e.g., aeolian and fluvial horizontal stratification, fluvial ripple stratification and aeolian tabular stratification), identified depositional environments and connected magnetic fabrics to that environment (e.g., gravity on horizontal plane, on slope, current, suspension and grain collision) using magnetic fabric parameters. The study also contains a summary about the interpretation of stereoplots and the alignment of the direction of principal susceptibility axes in relation to depositional processes and various sedimentary environments (Taira, 1989; p. 75). Although some of the results obtained from the investigation of loess succession are debated, the study and the applied analytical methods (e.g., Taira-plot) may help to describe the (re)depositional processes and environment of the dust (Bradák et al. 2018a).

Similar to the investigations of sedimentary magnetic fabric described above, the following studies are not conducted on loess successions but are related to processes that may appear during the alteration of loess after the deposition. One of the processes that may significantly change the sedimentary fabric is reworking by bioturbation (e.g., root activity and sediment transport within burrows dug by animals).

The research of Von Rad (1970) was one of the first to summarise the observations on the effect of bioturbation on sedimentary magnetic fabric. By drilling cores and comparing results with sediments deposited under known condition, Rees et al. (1982) concluded that bioturbation, which was clearly evident, does not always alter the primary sedimentary fabric. Based on the comparison of the

magnetic fabric that originated from natural and experimental sediments without and with evidence of bioturbation, Ellwood (1984) concluded that secondary physical processes (water flow and gravitational settling) play more significant roles in the reformation of the primary (here sedimentary) fabric compared to the minimal effect of biological activity. Flood et al. (1985) suggests that bioturbation weakens anisotropy and can be identified by various fabric parameters, such as the increasing dip of the foliation plane, strengthening lineation compare to foliation and the scattering alignment of principal susceptibilities in the stereoplots.

Along with bioturbation, which frequently appears in paleosols in terrestrial environments, additional pedogenic processes may play a significant role in the alteration of sedimentary fabric triggered by physical disturbance (e.g., vertical infiltration of groundwater), chemical alteration (e.g., weathering, sesquioxide, and Al/Fe oxide formation) and mineral neoformation (resulting from, e.g., bacterial activity). Despite the significance of such processes, the identification and description of their mark in the fabric of paleosols is still not the focus of (loess) anisotropy studies. Only a few studies have specifically focused on the effect of weathering on the primary fabric. Mathé et al. (1997) describes the change in magnetic parameters, including the magnetic fabric formed by lateritic weathering. In the studied cases, significant changes in the fabric parameters (degree of anisotropy and the shape parameter) were detected due to sapolitization (a weathering process that causes the absence of primary high susceptibility minerals), ferralitization (a strong weathering process that enhances susceptibility and sesquioxide formation) and maghemitization. The former (sapolitization) preserves the initial magnetic fabric inherited by the primary material, whereas the latter two change the character of the magnetic fabric. Sesquioxide formation homogenizes the fabric and the degree of anisotropy decreases to zero or approximately zero. Maghemite formation also reduces the degree of anisotropy and scatters the anisotropy directions (Mathé et al. 1997, 1999).

Nano scale single domain (SD) magnetic minerals may form during pedogenesis and can cause the appearance of an inverse magnetic fabric in loess successions. The term inverse magnetic fabric

was originally used by Rochette (1988), who identified the c-axis-preferred orientation of ferroan calcite (e.g., siderite) in which the maximum susceptibility is parallel to the c-axis; the term refers to “...a magnetic susceptibility ellipsoid whose maximum axis correspond to the minimum axis of the petrofabric...” (Rochette, 1988; p. 229). In SD particles, the minimum susceptibility axis is parallel to the long axis of the grain as well (Hrouda, 1982; Jackson, 1991); however, this topic remains poorly resolved (Parés, 2015, and the references therein). As shown below, the main of the research of magnetic fabric studies is whether the “inversion” is caused by the appearance of e.g., SD minerals and/or environmental processes.

### 1.1 Magnetic fabric studies of loess from the Chinese Loess Plateau to Alaska

Following the pioneering study of Heller et al. (1987) in the Luochuan section (Chinese Loess Plateau (CLP)), Liu et al. (1988) made one of the first steps in the investigation of the magnetic fabric of loess. In their study, AMS parameters were used to distinguish aeolian and water-lain materials originating from Xifeng loess. The studies of Heller et al. (1987), Liu et al. (1988), Thistlewood and Sun (1991) and Sun et al. (1995; in Chinese) were forgotten until the early 2000s when numerous magnetic fabric studies were performed on loess outcrops.

Zhu et al. (2004) (along with Lagroix and Banerjee 2002 and 2004a) opened a new chapter in the study of the loess fabric. These studies used various anisotropy parameters (e.g., F12, F23, and E12 -  $\epsilon_{12}$ ) to evaluate the statistical significance of lineation and foliation to verify the orientation of transportation found in the fabric (Section 3.). Along with the reconstruction of the prevailing wind direction, Zhu et al. (2004) used anisotropy parameters as a climate proxy, analysed their change through glacial and interglacial phases (from marine isotope stage MIS6 to 2) and compared them to frequently used magnetic proxies, such as frequency-dependent magnetic susceptibility ( $X_{fd}$ ).

Along with the determination of the wind direction during the winter and summer monsoon periods, Zhang et al. (2010) provided a model for fabric forming processes in loess (Baicaoyuan,

Xifeng and Yichuan successions; more information about the magnetic fabric-forming models can be found in Sub-section 4.4.1).

Following the studies that successfully reconstructed prevailing paleowind direction from the CLP (Sun et al. 1995; Zhu et al. 2004; Zhang et al. 2010), Liu and Sun (2012) came to a surprising conclusion from high-resolution sampling and studies of Luochuan loess. Specifically, the magnetic fabric of the Luochuan loess is influenced by various factors, such as particle size, compaction and pedogenesis, and no prevailing wind direction could be reconstructed from the random distribution of grains.

Ge et al. (2014) studied loess sections and developed on different paleoslopes at different sites during the Last Glacial (including the problematic Luochuan section). In contrast to the conclusion of Liu and Sun (2012), Ge et al. (2014) verified the role of loess MF in the reconstruction of prevailing wind direction. Instead of reflecting large-scale atmospheric circulation patterns, the wind direction seemed to be controlled by regional surface wind flow and influenced by regional topography. As a verification of the study of Ge et al. (2014) on the connection among MF, surface wind and regional topography, Peng et al. (2015) found significant, non-climate related changes in surface wind direction by analysing the fabric of Caotan succession (NE margin of the Tibetan Plateau). The results from MF analysis combined with a microtextural study of grains indicate that the change in regional topography (uplift of Tibetan Plateau) and the consequent cooling are factors responsible for the coeval changes in atmospheric circulation and dust source areas.

In one of the newest MF studies from Chinese loess, Xie et al. (2016) focused on the Neogene/Quaternary transition and found significant changes in Asian monsoon variation. This change, which was recorded in the Lantian loess section, may explain the trend towards increased aridity during that time.

Recently, a tendency in the displacement of the focus of loess research from CLP towards Central Asia has been noted. This tendency is reaching the field of magnetic fabric research as well. The analysis of Cheng et al. (2019) indicated prevailing near-surface SE wind around MIS3, while a

characteristic SW wind developed during MIS3b in the Tacheng area (Xinjiang region, NW China). This 'anomalous' wind was connected to the intensification of an anticyclone that formed over the area of growing glacier cover in the western and central Tianshan Mountains.

Among the earliest studies outside of the CLP, the magnetic fabric study of the Siberian loess provided a raw model for numerous subsequent studies. The goal of the study by Matasova et al. (2001) was to "test the conflicting viewpoints concerning the origin of the loess deposits at Kurtak loess" (Siberia) (Matasova et al. 2001; p. 377) by characterizing the MF. Following this analysis, no consensus was achieved on the sedimentary MF formation process in Kurtak loess. Various processes, such as aeolian sedimentation, solifluction, colluvial processes and water flow, seemed to develop similar fabrics. As a summary, Matasova et al. (2001) concluded that regardless of the origin of the orienting mechanism, the changing orientation of the fabric might indicate differences in prevailing transport directions during different glacial and interglacial periods. In addition, the study reported that pedogenic processes could alter the primary sedimentary magnetic fabric (i.e., development of isotropic fabric).

Extending the research by assessing more loess successions in SW and central Siberia, Matasova and Kazansky (2004) provided deeper insight in the mechanism of loess deposition and alteration. Based on their observation, the MF of unaltered loess (primary sedimentary fabric) reflects paleowind directions, which has generally not changed since the end of the Middle Pleistocene. In contrast, the study suggests that the alignment of the grains is a sensitive indicator for the degree of pedogenesis in paleosols. As a predecessor of Ge et al. (2014; see above), Matasova and Kazansky (2004) connected the regional differences in wind direction with different landscape positions of the studied successions (i.e., leeward and windward slope positions).

The earliest MF studies in the European Loess Belt (ELB) were performed in various profiles of Tönchesberg loess in Germany (Reinders and Hambach, 1995) and the Lower Danube Basin in Bulgaria (Jordanova et al. 1996). The goal of the former study was to identify the Blake magnetic excursion, and the supporting measurements characterized the magnetic fabric as having a random

distribution of grain orientations on the horizontal plane. The latter study mainly focuses on the sampling technique and warns about the possible deformation of fabric from inadequate sampling practices. The study briefly discusses the potential of magnetic fabrics in paleoenvironment reconstruction, i.e., reconstruction of prevailing wind directions and indications of bioturbation (random orientation of grains in paleosols).

The study of Hus (2003) built a bridge between various profiles from the western part of ELB (Kesselt and Remicourt, Belgium) through the East European Plain (Roxolany, Ukraine) and Siberia (Kurtac/k) towards the CLP (Huangling, Wucheng Formation). The study concludes some fundamental points about the fabric of loess, but unfortunately some of these points seem to fall into oblivion. Along with some observations, e.g., about the influence of bioturbation and the neoformed magnetic components in paleosols, the study focuses on the bedding plane parallel magnetic foliation and scattering orientations of magnetic lineation along the foliation plane (i.e., more likely isotropic than anisotropic fabric), as well as the role of phyllosilicates in the loess characterized by low magnetic susceptibility (Hus, 2003). Despite doubts about the feasibility of the identification of one process (i.e., the direction of transportation) of the numerous influences during the loess fabric formation (raised by the study of Huss, 2003), an increasing number of studies appeared to use magnetic fabric analysis as a tool to identify paleowind direction.

During the study of loess from Poland and western Ukraine, Nawrocki et al. (2006) focused on the marks of imbrication in the fabric supported by the lineation of magnetic grains lying in the direction of paleowind. The dip of the magnetic grains and the fabric (i.e., the dip of the foliation) was successfully applied as an indicator of imbrication and subsequently the paleowind direction in the Late Pleistocene. In some recent studies of loess profiles in Ukraine (Cherepyn, Roxolany and Koroshiv), Nawrocki et al. (2018, 2019) combined magnetic fabric investigation and absolute age dating (U-Pb ages of detrital zircon) to determine paleowind direction and the possible source area of the dust. The studies successfully connected the change of anisotropy parameters and the

paleowind direction to the fluctuation of the Fennoscandian ice sheet during the Last Glacial Maximum (Late Pleistocene) (Nawrocki et al. 2018, 2019).

A series of studies focused on Middle Danube Basin loess. First in the region, Bradák (2009) used MF orientation to reconstruct Middle Pleistocene paleowind direction. In further studies from Hungarian loess (Cérna Valley loess, Hungary), the formation and transformation of the fabric was reconstructed and connected to glacial and interglacial periods by the identification of characteristic processes, such as aeolian sedimentation (glacials), pedogenesis (interglacials) and erosion and redeposition by sheet-wash (transition periods) (Bradák et al. 2011, Bradák-Hayashi et al. 2016). Recent studies focused on the classification of loess variations by statistical analysis (hierarchical cluster analysis) of the magnetic fabric characteristics (Bradák and Kovács, 2014) and the influence of depositional and post-depositional process during loess fabric development (Bradák et al. 2018a, b and 2019a).

Zeeden et al. (2015) used anisotropy parameters to characterize the paleoenvironment during the Gravettian archaeological period at the Krems-Wachtberg archaeological site (Austria). Bösken et al. (2019) applied magnetic fabric analysis to reconstruct paleowind direction during the MIS3/2 transition as a part of a complex geoarchaeological investigation on Gravettian population in the Carpathian Basin (Bodrogkeresztúr section, Hungary).

Song et al. (2018) executed MF investigations as a part of the revision of the paleomagnetic results from Titel-Stari Slamen loess section (Serbia).

Obersteinova (2016) and Hrouda et al. (2018) are the first to perform magnetic fabric studies on loess successions from Moravia and Bohemia (Bulhary, Červený Kopec, and Tunel Blanka; Czech Republic). The former (Obersteinova, 2016) analysed the fabric to identify various surface processes during the development of the studied loess profiles. The latter study (Hrouda et al. 2018) is an introduction and application of new methods, namely, frequency-dependent magnetic susceptibility (fdAMS) and anisotropy of out-of-phase magnetic susceptibility (opAMS) measurements in loess (Sub-section 3.2).

Another significant study assessed the western part of the ELB. Compared to the pioneering study of Hus (2003) that introduced some fabric from Belgian profiles, Taylor and Lagroix (2015) focused on the detailed, high-resolution study of the Nussloch section (Germany) and specifically the formation and alteration of the sedimentary fabric.

A series of studies from Halfway House and Gold Hill Steps loess (Alaska) provide a 'raw model' for magnetic fabric studies of loess (Lagroix and Banerjee 2002, 2004a, b). Along with successfully identified systematic changes in prevailing wind directions linked to the rhythm of glacial and interglacial periods (Lagroix and Banerjee 2002), Lagroix and Banerjee (2004a) recommend a method of analysis to evaluate sampling induced deformation and isolate samples with statistically significant fabric orientation (Sub-section 3.3.2). Along with the primary aeolian fabric, Lagroix and Banerjee 2004b discovered a new type of magnetic fabric (axial oblate and prolate magnetic fabric) that was formed by the chain of events connected to permafrost activity.

Along with studies focusing on environmental reconstruction, a few studies on loess have been methodological or experimental in nature. Together with various rock samples, Jordanova et al. (2007) used loess samples to investigate the influence of stepwise alternating field (AF) demagnetization on various magnetic parameters, including e.g., the degree of anisotropy of magnetic susceptibility. The change in such parameters draws attention to the bias and the danger of data misinterpretation if the anisotropy measurements occur after AF demagnetization experiments.

The aim of the experiments executed by Wang and Løvlie (2010) was not to study the formation of loess MF but to "elucidate factors controlling the acquisition of magnetization in loess" (Wang and Løvlie, 2010; p. 394). Their experiments provided significant information about the character of a magnetic fabric that was developed during dry deposition in a laboratory environment.

As noted above, numerous fundamental points from loess magnetic fabric studies have already been established. The goal of this study is to summarize the significance and limitations of magnetic

fabric analysis of loess and introduce some novel results that may provide new perspectives in future studies.

## 2. Materials

### 2.1 A short introduction to loess

Loess variations cover approximately 10% of the Earth's land surface and play significant roles in terrestrial climate reconstructions from the Quaternary (Pye 1987).

Loess (*sensu stricto* aeolian loess) can be defined as an aeolian sediment that has been transported and deposited by the wind and is dominated by silt-sized (2-50  $\mu\text{m}$ -diameter) particles but also contains measurable amounts of sand and clay grain size particles. Loess can be recognized as a distinctive sedimentary body ranging from a few centimetres to several hundred metres in thickness (Muhs, 2007). The primary sedimentary structure of loess is homogenous and massive, and occasionally primary bedding structures, e.g., horizontal laminations and rare crossbedding, also appear. The coarser grains are cemented by finer interparticle clays and/or secondary carbonate as matrix (Muhs, 2007).

The term loess (*sensu lato*) has not been limited to the aeolian type introduced above. The formation of loess variations can be connected to various surface processes, such as reworking (e.g., bioturbation via root activity and burrows), pedogenesis, redeposition (e.g., by slope and water-lain surface processes) and deformation (e.g., compaction, cryogenic and seismic processes).

In addition to studying the forming environment of aeolian loess, understanding the alteration of primary aeolian material plays an important role in characterization of the paleoenvironment. The observation of the rhythmical alteration of loess and paleosol horizons led to further investigations, e.g., rock magnetic studies (magnetic susceptibility -  $X_{if}$ , and frequency dependence of magnetic

susceptibility  $X_{fd}$ ) and the development of two fundamental theories about the magnetic enhancement of loess (Evans, 2001). In loess sequences, sediments are generally characterized as low  $X_{if}$  and  $X_{fd}$ , and paleosols are generally characterized high  $X_{if}$  and  $X_{fd}$ . The so-called superparamagnetic (SP) minerals are indicated by high  $X_{fd}$  compared to multidomain (MD) and stable single domain (SSD) grains. Maher and Taylor (1988) discovered that the origin of such nanoscale SP components is related to biogenic processes strongly connected to pedogenesis. Therefore, the method of magnetic enhancement of primary loess by biogenic processes and weathering in paleosols is called the pedogenic model (Evans, 2001) (e.g., CLP and the ELB). In contrast, an increasing input of coarser magnetic particles by stronger winds causes an increased  $X_{if}$  in loess compared with that found in paleosols (Begét and Hawkins, 1989). This feature is called the wind vigour model (typical e.g., in Alaskan and Siberian loess) (Maher, 2018).

Repeating sedimentation, alteration of loess to palaeosol units and the deposition of new loess horizons, i.e., the evolution and cycles of loess successions, are connected to astronomical (e.g., solar insolation) and terrestrial (e.g., change in global ice volume) forces (Liu and Ding 1993, 1998; Ding et al. 1995; Liu et al. 1999).

These fundamental components of loess research, such as the origin, formation and alteration processes of loess and their use as climate proxies, significantly influence magnetic fabric studies as well.

## 2.2 Case study from Paks – Site and sampling

Along with some earlier results published in Bradák (2009), Bradák et al. (2011) and Bradák and Kovács (2014), magnetic fabric of samples from the Paks loess succession were analysed in this study (Suppl. Mat. 1). The Paks loess profile is located to the north of the town of Paks in the Pannonian Basin, Hungary and on the right bank of the Danube River. As a part of the ELB, the Paks succession plays an important role in terrestrial paleoclimate reconstruction in Europe (Újvári et al. 2014;

Marković et al. 2015) (Fig. 2). As part of a recent paleoenvironment study of Paks, a 16-m-thick loess/paleosol sequence was cleaned and subjected to high-resolution sampling, and various magnetic studies were conducted (Bradák et al. 2018a, b) (Fig. 2b).

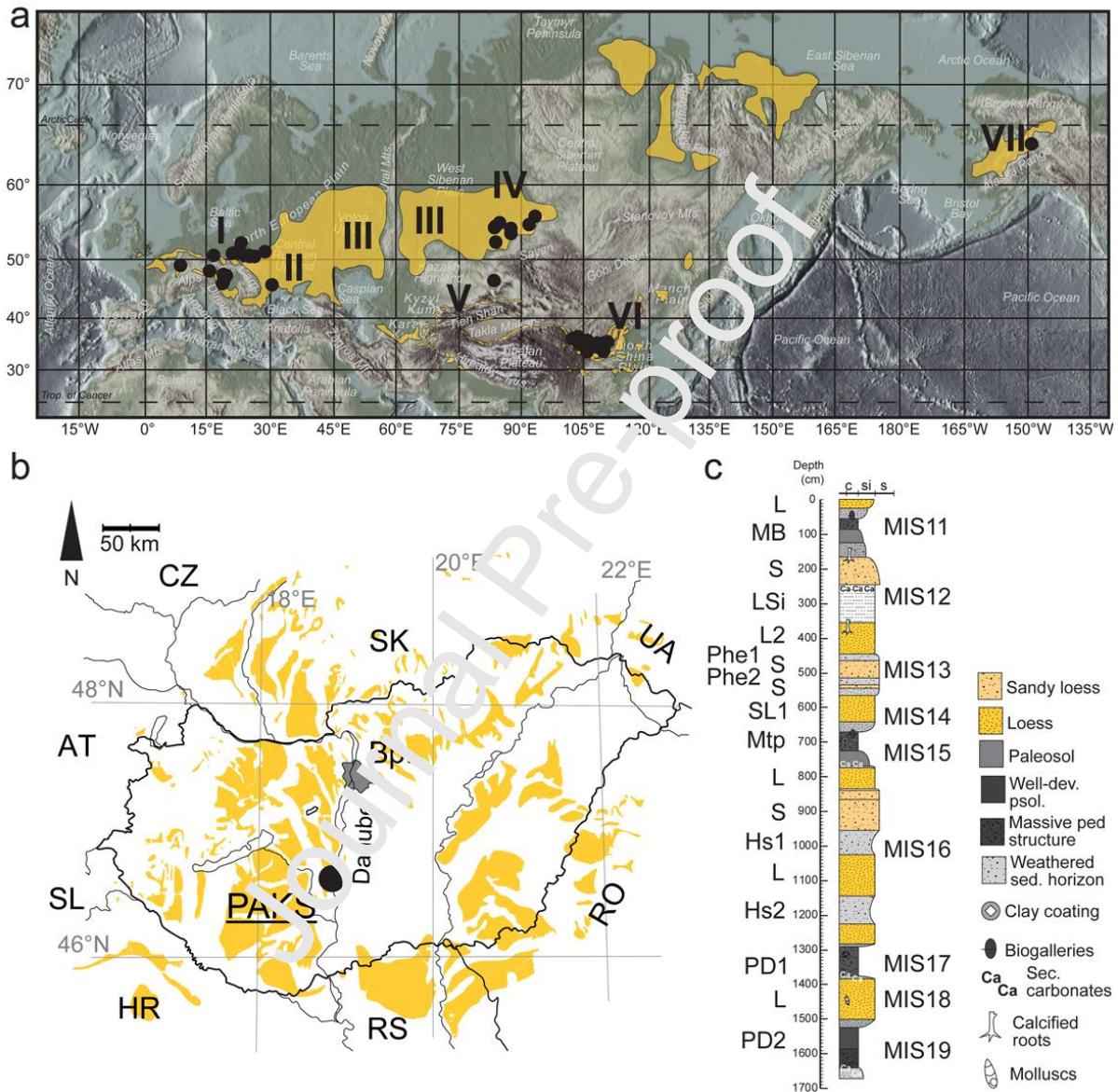


**Figure 2.** a) Schematic map of the distribution of loess in the Northern Hemisphere and the locations of the profiles appearing in the study, b) location of the Paks profile in Hungary, and c) the graphic log of the studied succession in the 2014-2016 research sessions. The yellow polygons in Fig. 2a and b indicate the schematic distribution of loess areas based on Haase et al. (2007), Muhs

(2007), Li et al. (2020) and Zan et al. (2020). I-European Loess Belt; II-Ukrainian Loess Belt; III-Russian Loess Belt with the IV-Siberian Loess; V-Central Asian Loess Region; VI-Chinese Loess Plateau and the VII-Alaskan Loess. The detailed list of the profiles (including e.g. references and coordinates) used in the map can be found in Supplementary Material 1. AT-Austria; CZ-Czech Republic; HR-Croatia; RO-Romania; RS-Republic of Serbia; SL-Slovenia; SK-Slovak Republic and UA-Ukraine. Fig. 2a and b is modified after Bradák et al. (2018a,b and 2019 b,c). The basic relief map is adapted from Amante and Eakins (2009). The chronostratigraphical subdivision of the section is based on Újvári et al. (2014).

The glacials, such as MIS 18, MIS 16, MIS 14, MIS 12 and MIS 10, were represented by various sediments in the studied sequence at the Paks abandoned brickyard (Fig. 2b). The loess (L), sandy loess (SL) and sand (S) sediment units were yellow and yellowish-grey in colour and consisted of fine-grained silt or silty sand with homogeneous or occasionally poorly developed fine laminated sedimentary structure. LSi is a laminated silt layer that was possibly deposited by water-lain processes (e.g., Fitzsimmons et al. 2014). L<sub>1</sub> is a well-sorted, grey, thinly laminated sediment with a parallel, wavy structure and contains a secondary carbonate between the laminas. The chronostratigraphical position of the unit remains unclear; however, it may date to MIS 12 (Újvári et al. 2014).

Interglacials, such as MIS 19, MIS 17, MIS 15, MIS 13 and MIS 11, were represented by various paleosols (Fig. 2b; Újvári et al. 2014; Marković et al. 2015), which are briefly summarized in Table 1 and detailed in Bradák et al. (2018b and 2019b, c).

Abbrev.	Name	Depth (m)*	Forming <sup>†</sup>	Correl. to CLP <sup>§</sup>	Colour (Munsell colour; moist/dry)	Characteristics
---------	------	---------------	----------------------	--------------------------------	---------------------------------------	-----------------

					Upper: brownish red (5YR4/4; 7.5YR5/4); lower: red (5YR4/4; 5YR5/4)	Well-dev.; angular blocky (upper) ped. struct. and, sandy-clayey (lower); B <sub>k</sub>
Phe1 and Phe2	Mende Base Paks Sandy Soil Complex	0.3-1.3 (Ph1); 5.1-5.6 (Ph2)	MIS11 MIS13	S4 S5	Slightly darker than the parent mat. (Ph1: 10YR5/4; 10YR6/4 and 7/4; Ph2: 10YR5/4; 10YR7/4)	Very weak, single grain ped. char.; appearance of small, ~0.5 cm diameter biogalleries
Mtp	-	6.5-7.8	MIS15	S5	Brown (2.5Y6/3; 2.5Y8/2)	Homogeneous; well-developed; massive ped. struct; B <sub>k</sub>
Hs1 and Hs2	('embryonic soils')	9.6-10.2; 11.5-12.2	-	S5 and S6	Slightly darker than its parent material.	Weathered horizons, very weak paleosol Clayey; well-
PD1	Paks Double 1	12.8-13.9	MIS17	S6	Red (7.5YR3/4; 7.5YR5/4)	developed; granular, angular blocky ped struct.; B <sub>k</sub>
PD2	Paks Double 2	15-16.7	MIS19	S7	Red (7.5YR5/4; 7.5YR6/4)	Clayey; massive, angular blocky soil structure; B <sub>k</sub>

\* Please see Fig. 2b

<sup>†</sup> Based on Újvári et al. (2014)

<sup>§</sup> Marković et al., (2015)

B<sub>k</sub>, (C<sub>Ca</sub>) - CaCO<sub>3</sub> accumulation horizon.

**Table 1.** A brief summary of the paleosol units of the studied loess successions. More detailed descriptions of the units are available in Bradák et al. (2018b, 2019b and c).

Oriented block samples (“hand-cut blocks”) approximately 10×10×10 cm in size were collected every 10-cm depth interval in the preliminary sampling of the Paks profile. Cubic specimens of 2×2×2 cm were cut from the block samples. No plastic holder was applied to avoid fabric deformation during sampling and sample preparation (Jordanova et al. 1996; Matasova et al. 2001). This method of sampling provided approximately 6 to 10 pieces of specimens from every sampled horizon, which meets the criterion for a statistically significant number of specimens, e.g., during the stereoplot analysis.

### 2.3 Case study from Paks – Material and mineral composition

During the magnetic anisotropy studies of loess, it is essential to know what types of minerals comprise the (magnetic) fabric. Loess contains fine grain aerosols travelling in regional/continental distance (e.g., Varga et al. 2016), coarser dust from local sources (e.g., Újvári et al. 2012; Thamó-Bozsó et al. 2014) and, as discussed above, neoformed minerals (Sub-section 2.1).

Examples from the Paks loess succession represent the characteristics of magnetic mineral composition in loess and paleosols (Bradák et al. 2018a, b and 2019b). Scanning electron microscope (SEM) observations (combined backscattered electron imaging and X-ray elemental scanning) of thin sections characterise the distribution of magnetic components in the microfabric of loess samples (Bradák et al. 2018a, b and 2019b).



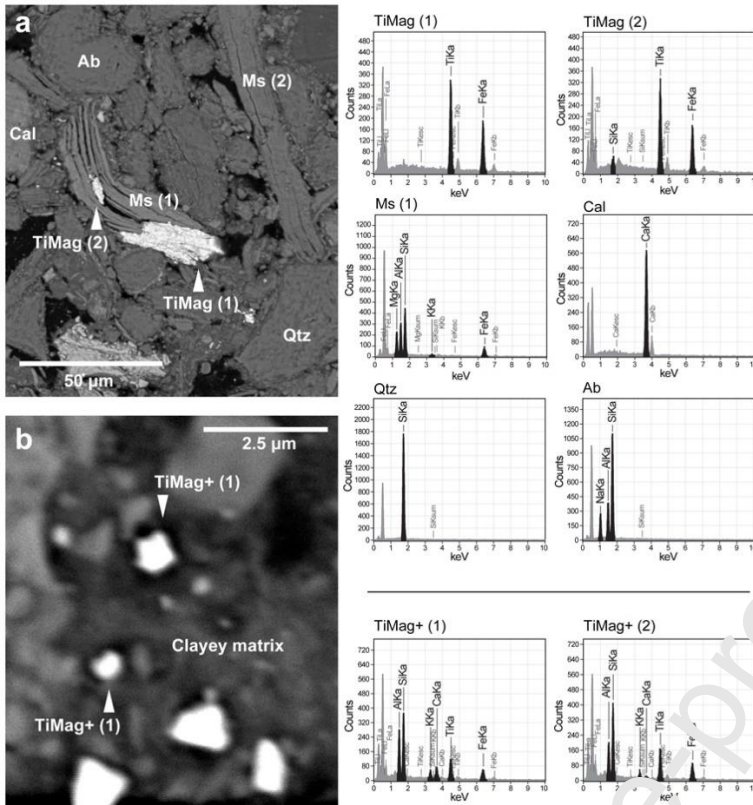


**Figure 4.** Microfabric of loess (a) and palaeosol (b) samples. Energy-dispersive X-ray spectroscopy (EDS) spectra of the indicated grains is presented to the right of the figures. Abbreviations are as follows: Ab – albite (plagioclase), Cal – calcite, Ms – muscovite, Qtz – quartz, TiMag – titanomagnetite. TiMag+ EDS spectra indicate a mixture of the signal of submicron size titanomagnetite and other mineral components (e.g., clay minerals) (due to the limitation of the instrument, no clear EDS spectra could be presented).

Energy-dispersive X-ray spectroscopy (EDS) revealed the mineralogical components of the samples (Fig. 4; and Bradák et al. 2018a, b and 2019b). Compared to the sporadic appearance of ferromagnetic minerals, such as iron oxides (most likely [titano]magnetite and haematite) and ilmenite, high amounts of paramagnetic phyllosilicates, such as muscovite (Fig. 3 and 4; Ms) and chlorite, were observed in primary aeolian sediments. Quartz and calcite (Fig. 3 and 4; Qtz and Cal) were the most common components that were present in relatively high amounts along with other contributors, such as albite, epidote, K-feldspar and rutile (Fig 3). The mineral composition of the

studied paleosols is similar to aeolian loess, suggesting a sedimentary origin of coarser grain components (Bradák et al. 2018a, b and 2019b) (Fig. 3).

The alteration of the original sedimentary fabric was indicated by the evidence of physical and chemical weathering: the appearance of fine grain components (clayey matrix) (Fig. 3c, d, e and f); the degradation of minerals, such as phyllosilicate sheet detachment (Fig. 4a); the fragmentation of coarser grains (Fig. 4b); and the compaction of the fabric (Bradák et al. 2018b and 2019b).

The results of the case study from the Paks are consistent with the general description of Muhs (2007): most loess deposits have mineralogy that includes quartz, plagioclase, K-feldspar, mica, calcite (and sometimes dolomite), and phyllosilicate clay minerals (smectite, chlorite, mica, and kaolinite). Heavy minerals are usually present but in small amounts (Muhs, 2007).

### 3. Methods

#### 3.1 Magnetic anisotropy measurements in loess

Anisotropy of low-field magnetic susceptibility (AMS), which is the most common method used in loess fabric studies, provides a useful tool to characterize the magnetic fabric of materials. The magnetic fabric, as characterized by AMS, reflects the alignment of magnetic contributors in the material that have preferred dimensional orientation (pdo) controlled by magnetic anisotropies and minerals with crystallographic preferred (crystallographic axis) orientation (cpo) controlled by magnetic anisotropies. Therefore, the magnetic fabric can provide potential insight into various processes, including the type and orientation of material transport, flow energy, post-sedimentary processes, and stress fields (Tarling and Hrouda, 1993). Due to its nature, AMS measurements reflect the orientation of all grains in the material, including e.g., paramagnetic contributors, which may bias the measurement results in samples with low magnetic susceptibility (e.g., Hus, 2003).

For sediments characterized by low magnetic susceptibility ( $\kappa_{f_{avg}} < 5 \times 10^{-4} \text{SI}$ ), paramagnetic components contribute significantly to the bulk magnetic susceptibility value (Rochette, 1987; Hrouda and Jelinek, 1990). In loess, which consists of a numerous paramagnetic contributors compared to ferromagnetic components (see Sub-section 2.2), the “bias” triggered by the anisotropy of paramagnetic minerals may become significant and makes the interpretation of the fabric orientation complex in loess (e.g., Hus, 2003; Taylor and Lagroix, 2015). As suggested by e.g., Rochette et al. (1992), Hus (2003) and Taylor and Lagroix (2015), the relationship between anisotropy degree and the mean magnetic susceptibility may help to reveal paramagnetic influence in loess. The lack of a relationship between the two parameters suggests that the AMS is controlled by the paramagnetic mineral fraction rather than ferrimagnetic contributors (Rochette et al. 1992; Hus, 2003; Taylor and Lagroix, 2015). Along with AMS, other magnetic anisotropy methods are available to study loess that may reveal additional information about the fabric (Bilardello and Jackson, 2014; Bilardello, 2016) and may help to separate the paramagnetic and ferromagnetic fabrics. To complete the AMS results, anisotropy of isothermal remanent magnetization (AIRM) experiments performed by Jordanova et al. (1996) identified SD or near SD states and multidomain (MD) magnetite and haematite grains in the fabric of Bulgarian loess. Hus (2003) examined the anisotropy of partial and total anhysteretic remanence (APARM and AARM) to compare the magnetic fabric influenced by paramagnetic contributors and identify the preferred orientations of the soft and hard ferrimagnetic fractions.

Along with paramagnetic contributors, the identification of magnetic fabric influenced and/or formed by mineral neoformation may represent a challenge during the study of loess successions. In loess/paleosol sequences, production of ultrafine magnetic particles in the transition between the superparamagnetic (SP) and stable single domain (SSD) states is mainly related to pedogenic processes, such as weathering and biogenic activity (Maher and Taylor, 1988; Forster et al. 1994); therefore, these particles can potentially bias the original primary sedimentary fabric and provide

fundamental information about pedogenesis. Due to its nature, i.e., built in situ with neoformed magnetic components, we propose the term “authigenic magnetic fabric”.

Following the extension of the limits of measuring methods (Pokorný et al. 2011), Hrouda and Ježek (2014) were among the first to note the potential of a new type magnetic anisotropy analysis in loess research: the determination of the anisotropy of frequency-dependent magnetic susceptibility (fdAMS). fdAMS analysis provides an easy method to separate the remains of the primary magnetic fabric and the authigenic pedogenic fabric, which consist of nanoscale (mainly SP/SSD) contributors.

Anisotropy of out-of-phase magnetic susceptibility (opAMS) has been recently developed for the identification of authigenic pedogenic fabric (Hrouda et al. 2018). Both fdAMS and opAMS are controlled by magnetic particles of similar sizes. Therefore, opAMS can indicate the preferred orientation of ultrafine pedogenic magnetic properties.

## 3.2 Analysis of the magnetic fabric

### 3.2.1 Magnetic fabric parameters

The output of anisotropy of magnetic susceptibility measurements is a second-rank tensor that can be conveniently visualized as a magnetic susceptibility ellipsoid with three mutually perpendicular principal susceptibility axes, namely,  $\kappa_{\max}$  (maximum susceptibility),  $\kappa_{\text{int}}$  (intermediate susceptibility) and  $\kappa_{\min}$  (minimum susceptibility), which are the three eigenvectors of the susceptibility tensor (Hrouda, 1982; Tarlin and Hrouda, 1993). The magnetic susceptibility ellipsoid defines the so-called magnetic fabric with magnetic lineation (orientation of the  $\kappa_{\max}$  axis) and magnetic foliation (plane containing  $\kappa_{\max}$  and  $\kappa_{\text{int}}$  axes and perpendicular to the  $\kappa_{\min}$  axis) (Fig. 1). The quantitative parameters that describe the magnitude and shape of the magnetic susceptibility ellipsoid can be defined using numerous methods (see, Table 1.1 in Tarling and Hrouda, 1993). Currently, the most commonly used quantitative parameters include the following: foliation (F),

lineation (L), corrected degree of anisotropy (Pj) and shape parameter (T). These parameters are used frequently in loess/paleosol research and can be calculated as it is summarised in Table 2.

Magnetic anisotropy parameter (abbrev.)	Equation (equation number in the text)	References
Foliation (F)	$\kappa_{int}/\kappa_{min}$ (Eq. 1)	Stacey et al. (1960)
Lineation (L)	$\kappa_{max}/\kappa_{int}$ (Eq. 2)	Balsey and Buddington (1960)
Corrected degree of anisotropy (Pj)	$\exp \sqrt{2[(\eta_{max} - \eta_m)^2 + (\eta_{int} - \eta_m)^2 + (\eta_{min} - \eta_m)^2]}$ (Eq. 3)*	Jelinek (1981)
Shape parameter (T)	$(2 \times \eta_{int} - \eta_{max} - \eta_{min})/(\eta_{max} - \eta_{min})$ (Eq. 4)*	Jelinek (1981)
Shape factor (q)	$(\kappa_{max} - \kappa_{int})/[0.5 \times (\kappa_{max} + \kappa_{int}) - \kappa_{min}]$ (Eq. 6) <sup>#</sup>	Granar (1958)

\* In the case of Eq. 3, 4 and 5:  $\eta_{max} = \ln \kappa_{max}$ ;  $\eta_{int} = \ln \kappa_{int}$ ;  $\eta_{min} = \ln \kappa_{min}$ ;  $\eta_m = \sqrt[3]{\eta_{max} \times \eta_{int} \times \eta_{min}}$

<sup>#</sup>Granar's shape factor was used during the study of Paks loess therefore it is listed in the chart.

**Table 2.** The summary of magnetic fabric parameters used in this study.

### 3.2.2 Statistical significance analysis of AMS parameters

Data verification after the measurements typically begins with the evaluation of F statistics (e.g., Jelinek, 1981; Lagroix and Banerjee, 2004a; Zhu et al. 2004). Lagroix and Banerjee (2004a) summarized the criteria for a primary fabric with a well-defined orientation (statistically significant  $\kappa_{max}$ ) for loess samples. An area of uncertainty around the orientation of principal axes is quantified by 95% confidence ellipses that have semi-axes, which are denoted by epsilon ( $\epsilon$ ). At the specimen level, the 95% confidence uncertainty ellipse of  $\kappa_{max}$  is defined by semi-axes  $\epsilon_{12}$  and  $\epsilon_{13}$ , where  $\epsilon_{12}$  is the half-angle uncertainty of  $\kappa_{max}$  in the plane joining  $\kappa_{max}$  and  $\kappa_{int}$ , and  $\epsilon_{13}$  is the half-angle uncertainty of  $\kappa_{max}$  in the plane joining  $\kappa_{max}$  and  $\kappa_{min}$ . The maximum allowable  $\epsilon_{12}$  of statistical

significance indicating well-oriented grains in individual samples is  $22.5^\circ$  (Lagroix and Banerjee, 2004a). In the other words, Zhu et al. (2004, p. 59) state that “ $E_{12}$  ( $\epsilon_{12}$ ) indicates the angular uncertainty in the direction of  $\kappa_{\max}$  within the magnetic foliation plane. Because the measured foliation is generally almost horizontal,  $E_{12}$  represents the 95% confidence angle for the azimuth of  $\kappa_{\max}$ ”. Samples with statistically significant lineation are defined by two parameters:  $F_{12} > 4$  and  $\epsilon_{12} < 20^\circ$ .

Correlations between  $\epsilon_{12}$  and anisotropy parameters, such as L, F, and Pj, verify the appearance of significant lineation in the samples (e.g., strong inverse relationship between  $\epsilon_{12}$  and L) (Lagroix and Banerjee, 2004a). The  $F_{12} - \epsilon_{12}$  plot, which was introduced by Zhu et al. (2004), can be studied for the same reason as L –  $\epsilon_{12}$  plot. Additional diagrams have been used for further evaluation. The relationship between F and F23 was also investigated by Zhu et al. (2004) to reveal well-resolved magnetic foliation in the fabric. Random measurement error in samples with low bulk susceptibility can be identified by the analyses of the relationship between  $F_{12}$  and bulk magnetic susceptibility (Zhu et al. 2004).

### 3.2.3 Frequently used plots in loess magnetic fabric analyses

Two frequently used and one less known plot are employed in these analyses and are introduced below. These diagrams have been commonly applied in anisotropy studies but do not seem popular in the study of loess; however, these diagrams may provide significant information about the forming environment of sediment and paleosol units. The most commonly applied plot in loess/paleosol studies is the Pj – T diagram (e.g., Liu et al. 1988; Jordanova et al. 1996; Matasova et al. 2001; Lagroix and Banerjee, 2002; Matasova and Kazansky, 2004; Bradák et al. 2011; Taylor and Lagroix, 2015; Bradák et al. 2018a, b, 2019; Nawrocki et al. 2019). For loess, the so-called Jelinek diagram introduced by Jelinek (1981) may be useful to distinguish various transport facies by exploiting the influence of transport/deposition energy or pedogenesis on the characteristics of the

magnetic fabric (alignment of the grains) as represented by the shape of the susceptibility ellipsoid (oblate or prolate).

The dominance of foliation or lineation on the magnetic fabric can be assessed using F – L or Flinn diagrams. Flinn diagrams were originally applied to describe the shapes of strain ellipsoids (Flinn 1962). Similar to the strain ellipsoid (used in structural geological studies), the shape of the susceptibility ellipsoid can be characterized by the relation between the F and L parameters plotted on a Flinn-like diagram (e.g., Zhu et al. 2004; Taylor and Lagroix, 2015; Bradák et al. 2011, 2018a). The dominance of F indicates an oblate ellipsoid and a flattening strain. In contrast, the dominance of L indicates a prolate ellipsoid and a constrictional strain. Similar to the Jelinek plot, the objective of using the Flinn diagram is that the F and L parameters can be analysed along with the shape of the susceptibility ellipsoid.

The  $q$  (shape factor) –  $\beta$  (imbrication angle) diagram was introduced by Taira (1989) to characterize the stresses and the transportation energy during fabric production.  $\beta$  is the inclination of the minimum principal susceptibility. In the case of Taira (1989), the angle of imbrication is defined by the tilt of the short axis. Grünert first applied  $q$  (1958) (Table 2).

The factor  $q$  compares the intensity of magnetic lineation in the magnetic foliation plane with the intensity of foliation (Taira, 1989). The  $q$  and  $\beta$  values are related to the gravitational and tangential stresses in fabric production. Based on the study of Taira (1989), various areas can be separated on the diagram based on the  $\beta$  and  $q$  values related to materials transported by various processes (e.g., gravitational, aeolian and water-lain), deposited in various environments (e.g., aeolian and fluvial), and characterized by various sedimentary structure (e.g., homogenous, laminated and cross-bedded). Although the Taira diagram can be potentially used to characterize the depositional energy of dust (Bradák et al. 2018a) or distinguish between units deposited in various sedimentary environments (e.g., aeolian and redeposited loess by water-lain processes), the appearance of high  $\beta$  in paleosols due to the reorientation of grains by vertical processes may cause some complications.

Liu et al. (1988) used P – L and P – F plots, correlation and analysis of the coefficient of the linear trend after correlation to separate undisturbed (i.e., aeolian, windblown) loess and redeposited (water-lain) materials. The adaptation of the method, e.g., by Bradák (2009), yielded promising results; however, a study of aeolian and redeposited loess using this method resulted in more question regarding the efficiency of the method (Bradák and Kovács, 2014).

### 3.2.4 Analysis of stereoplots

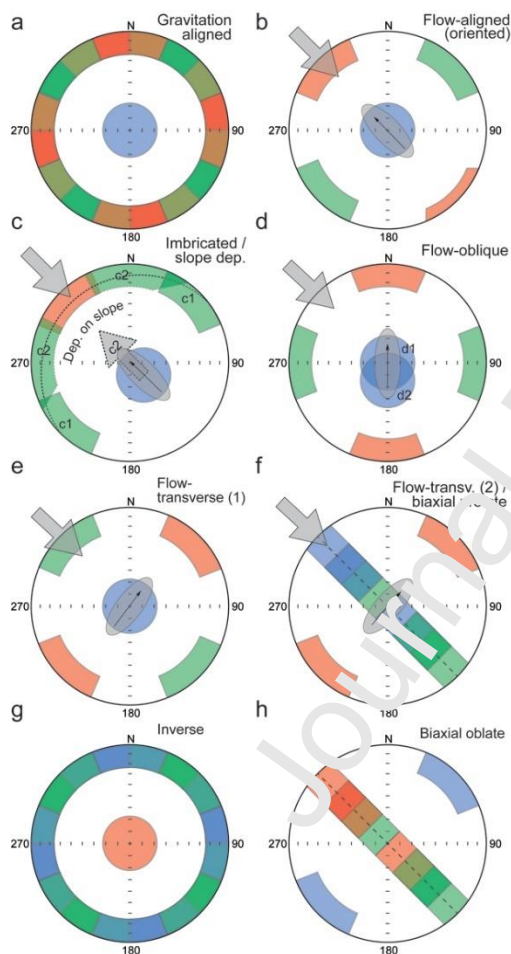


**Figure 5.** Magnetic fabric types observed in sedimentary facies. The red, green and blue coloured areas represent the theoretical distribution of the directions of  $K_{max}$ ,  $K_{int}$  and  $K_{min}$  axis, respectively. The grey arrows and the grains with small black arrows indicate the relationship of paleocurrents and the alignment of grains with preferred dimensional orientation. In Fig 5c, c1 area indicates the theoretical distribution of the imbricated fabric, and the c2 arrow represents the orientation of

magnetic lineation in the deposition on slope. The dotted line indicates the dip of the foliation plane compared to the horizontal orientation. In Fig 5d, d2 area indicates potential imbrication as demonstrated by the discrepancy of magnetic foliation from the horizontal (for a detailed description of various types and references, please see Sub-section 3.2.4).

One of the commonly used analytical methods in anisotropy studies is the application of stereoplots, i.e., the stereographical projection of the directions (declination and inclination) of principal susceptibility axes. The orientation of principal susceptibilities reflects the orientation of the susceptibility ellipsoid, and the alignment of magnetic contributions can be easily visualized in this manner. Various types of magnetic fabric can be classified by the distribution of principal susceptibility axes on stereoplot. The main magnetic fabric types, introduced below, can be observed in various sedimentary successions formed in aeolian, fluvial, alluvial and marine environment, including loess-paleosol records (Fig. 5).

During the formation of gravitation-aligned fabric (e.g., Taria, 1989; Tarling and Hrouda, 1993; “horizontal fabric” in Baas et al. 2007) (Fig. 5a), gravitational and magnetic forces are the only operating forces that result in a random scattering of grains in the foliation plane. The gravitationally aligned fabric displays quasi-horizontal foliation with a dip of a few degrees and scattered alignment of magnetic lineation ( $\kappa_{\max}$  axes) in a horizontal plane without any characteristics of fabric orientation. Such a sedimentary magnetic fabric may form in an environment with no current flow. Along with gravity, magnetic forces may orient very fine grains ( $<1 \mu\text{m}$ ) following the alignment of local geomagnetic field (Tarling and Hrouda 1993).

If currents are present during the deposition, a flow-aligned magnetic fabric can be developed (Fig. 5b). In the flow-aligned fabric, elongated grains tend to align parallel with the transport direction and may show an up-flow tilting. In weaker currents ( $<1 \text{ cm/s}$ ), the tilting is less than  $10^\circ$ . In the case of stronger currents ( $\geq 1 \text{ cm/s}$ ), a  $5\text{--}20^\circ$  dip in the magnetic foliation plane is clearly indicated by the deviation of  $\kappa_{\min}$  from the vertical orientation (Tarling and Hrouda, 1993). The dip of

magnetic foliation was defined as a marker of imbrication of magnetic particles and used to infer paleowind directions by Nawrocki et al. (2006) (Fig. 5c1). Unfortunately, a similar magnetic fabric can develop if sedimentation occurs on a slope. The dip direction of the slope can be identified by the alignment of principal susceptibility axes; the tilt of  $\kappa_{\min}$  directions from the vertical and inclination of the plane is defined by the intermixing of  $\kappa_{\max}$  and  $\kappa_{\text{int}}$  from the horizontal plane (Rees 1966, 1971) (Fig. 5c2).

In the ideal flow-aligned and imbricated magnetic fabric, the well-clustered magnetic lineation distributed along the foliation (imbrication) plane may indicate a-axis imbrications and clearly defines the orientation of the currents (Fig. 5b and c1). Overall, gravitational force still dominates the depositional environment (stronger than the tangential force), which creates (strongly) an oblate magnetic fabric within the bedding plane (Tarling and Hrouda, 1993). Such a magnetic fabric is reported in the research of, e.g., Rees (1968), Rees and Woodall (1975), Taira (1989), and Baas et al. (2007).

Contrary to the flow-aligned fabric magnetic lineation can be oriented at  $\sim 45^\circ$  clockwise or anti-clockwise to the paleoflow direction (Fig. 5d). This phenomenon is referred to as a flow-oblique magnetic fabric and can be identified by the characteristic discrepancy of  $\kappa_{\max}$  and the dip of the foliation plane. The imbrication and the bi-directional (re)orientation of the elongated grains may be developed by the combined influence of stronger currents and gravity during settling on inclined surface (slope) (Fig. 5d2). Formation on the flow-oblique fabric can be found in studies from Rees (1966), Rees and Woodall (1975), Taira (1989) and Baas et al. (2007).

Two types of magnetic fabrics have been defined as flow-transverse magnetic fabric (or biaxial prolate, AB plane imbricated, pencil and “rolling” fabric) in the literature. In the first type, the a-axes of clasts, which are represented by  $\kappa_{\max}$ , are aligned perpendicularly to the flow direction, and the intermediate axes ( $\kappa_{\text{int}}$ ) are aligned in the flow direction. The orientations of principal susceptibilities are well separated, and current orientation is indicated by a 10–20° dip of magnetic foliation plane (perpendicular to  $\kappa_{\min}$ ) and the orientation of intermediate magnetic susceptibility (e.g., Baas et al.

2007) (Fig. 5e). In the second type, the flow-transverse fabric is characterized by well-clustered  $\kappa_{\max}$  directions, and the  $\kappa_{\min}$  and  $\kappa_{\text{int}}$  axis create a girdle perpendicular to the  $\kappa_{\max}$  axis (across the foliation plane). (Fig. 5f). The development of magnetic fabric is potentially indicates strong currents, traction and rolling of grains during transportation and a stable condition after deposition (Rees, 1983; Tarling and Hrouda, 1993; Tauxe, 1998; Lagroix and Banerjee, 2004b). In both types, the transport direction is perpendicular to the orientation of  $\kappa_{\max}$ .

A quasi-vertical magnetic foliation plane compared to the (theoretically) quasi-horizontal sedimentary plane, i.e., high plunge of  $\kappa_{\max}$  (and low plunge of  $\kappa_{\min}$ ) axes, may indicate “true” inverse fabric (triggered by the physical property of the grains, e.g., Parés, 2015 and references therein) and/or “mechanical” inverse fabric (i.e., vertically oriented grains compared to the assumed horizontal sedimentary plane caused by various geological/pedological processes) (Fig. 5g). A “true” inverse magnetic fabric can be formed by SD magnetic grains (Hrouda, 1984; Parés, 2015 and references therein) for which the susceptibility of the easy axis (the longest dimension of an elongated grain) is basically zero because the magnetization in this direction is already saturated; the distribution of the longest axes of SD grains thus defines the minimum susceptibility direction ( $\kappa_{\min}$ ). A mechanical inverse fabric (vertically oriented fabric) can be formed by various processes (e.g., bioturbation, pedogenesis) and is summarized below.

The stereoplot of biaxial oblate fabric is characterized by well-clustered  $\kappa_{\min}$  directions, and  $\kappa_{\max}$  and  $\kappa_{\text{int}}$  create a girdle perpendicular to the  $\kappa_{\min}$  direction. This fabric is rare in undeformed sediments. Among the studied loess profiles, it was only identified in two sections (Lagroix and Banerjee, 2004b; Bradák et al. 2019a), and various explanations describe their formation (Section 4) (Fig. 5h).

### 3.2.5 Cluster analysis

The distribution of quantitative anisotropy factors can be evaluated by means of multivariate statistics. The scope of such classification methods is to group and compare the studied (loess)

samples based on their similarity and common properties (i.e., anisotropy parameters, such as F, L, Pj, and T). One of the preferred multivariate methods is cluster analysis, the results of which can be visualized on a dendrogram.

Clustering is a method of coding in which samples from various units of loess succession that were originally described with many parameters (i.e., quantitative anisotropy parameters) are now described by only one value, its group code (cluster number, cluster group number). During clustering, the number of samples is decreased by placing the similar ones into groups (instead of decreasing the number of parameters) (i.e., samples with similar anisotropy parameters will fall into the same cluster group). It is an important criterion that every sample has to belong to a group but only to one group. The main aim of cluster analysis is to settle the similar samples (samples characterized by similar anisotropy parameters) into the same group; however, the complexity is derived from the fact that there are not only one group of conformations. "Cluster analysis (CA) classifies a set of observations into two or more mutually exclusive "unknown" groups based on combinations of interval variables. The purpose of cluster analysis is to discover a system of organizing observations, usually people, into groups, where members of the groups share properties in common" (Stockburger, 2001). In the case of magnetic fabric analysis, the created cluster groups may reveal characteristic magnetic fabric types related to various sedimentary and pedogenic environment.

Following the cluster analysis, it is important to verify the correctness of grouping and the existence of the definite groups using various methods. Discrimination analysis can be applied to test the cluster analysis results. During discriminant analysis, the samples are taken to such a discrimination field, where the separation is optimal. The analysis reveals the extent to which the planes separating the groups can be distinguished by building a predictive model for group membership. The model is composed of a discriminant function (a set of discriminant functions for more than two groups) based on linear combinations of the predictor variables that provide the best discrimination between the groups. Discriminant analysis results are often visualized on the surface

stretched between the first two discriminating planes (functions 1 and 2) (e.g., Afifi et al. 2004; applied in loess magnetic fabric: Bradák et al. 2011; Bradák and Kovács, 2014).

Calculation of Wilk's lambda coefficients ( $\lambda$ ) helps to determine the (degree of) influence of parameters (i.e., the anisotropy parameters) on the formation on each created sample group. Here,  $\lambda$  always falls between 0 and 1. If  $\lambda = 1$ , then the mean of the discriminant scores is the same in all groups, and there is no intergroup variability. Thus, in our case, the anisotropy parameter does not affect the formation of the cluster groups (Afifi et al., 2004). If  $\lambda = 0$ , then that particular parameter affects the formation of the cluster groups the most, i.e., this (anisotropy) parameter shows significant differences between the cluster groups and may indicate different forming environments. The smaller the quotient, the more it determines the formation of the cluster groups (Bradák and Kovács, 2014). The first application of cluster analysis on magnetic fabric parameters in loess studies showed promising results at the separation of sedimentary and pedogenic units from loess successions (Bradák et al. 2011), but the results of further measurements did not fully meet expectations (Bradák and Kovács, 2014).

### 3.2.6 Wavelet spectrum analysis

Wavelet spectrum analysis (WSA) can be employed on high-resolution data to investigate the existing periodicity in the series. Since it is localized over both time (space) and scale (frequency), it is possible to capture those characteristics that change over time (periodicity). The basis of WSA is a continuous wavelet transform (CWT; Eq. 6), which may be defined as the convolution of the data and the wavelet function (Kovács et al. 2010) of a given time series ( $X_n$ ,  $n = 1, \dots, N$ ) possessing equal time intervals  $\delta t$ , (Eq. 6). The WSA is a function of mean zero that is localized in both frequency and time (Grinsted et al. 2004).

$$W_n^X(S) = \sqrt{\frac{\delta t}{S} \sum_{n'=1}^N X_{n'}} \Psi_0 \left[ (n' - n) \frac{\delta t}{S} \right] \quad (\text{Eq. 7})$$

where  $s$  is the scale,  $\psi_0$  is the wavelet function, and  $\delta_t$  is the degree of resolution.

In this study, a Morlet mother wavelet (Morlet et al. 1982) yielded the source function from which daughter wavelets could be generated. This was achieved via the scaling and transformation of the mother wavelet. The degree of adaptability of the WSA enables it to address the problem of nonstationarity (Daubechies, 1990). The purpose of the wavelet transformation is multiple dissociation, which is achieved by decomposing the data in the scaling space. Thus, it possible to visualize its self-similarity structure (Farge, 1992; Kovács et al. 2010). Given that the wavelet spectrum is composed of independent time and frequency variables, its visualization in 3D is possible by plotting power spectrum density (psd) graphs. Since a more in-depth discussion of the WSA is not especially relevant here, the following publications are suggested to provide more information about its use: Benedetto and Frazier (1994) and Vidakovic (2009).

Due to missing data, the time interval is not always equidistant, and a spline interpolation can be applied. High-degree polynomials may be used in spline interpolation, and these polynomials must pass through every measured data point. Then, the polynomials are resampled to compensate for the missing data. In the present case (Section 5), a cubic polynomial was applied (Lyche and Schumaker, 1973). All the mathematical computations were performed using R 3.2.3 (R Core Team, 2015), and the WSA was conducted using the dplr package (Bunn, 2010; Bunn et al. 2016). Despite the broad range of application of WSA in Earth science (in loess research: Heslop et al. 2002; Basarin et al. 2014; Song et al. 2014), WSA has not been applied on AMS parameters from loess successions.

### 3.2.7 Return maps

For example, the series of anisotropy parameters sampled continuously from a succession, every member of the series ( $n, n+1, n+2...n+i$ ) represents one moment in time. The map (plot) in which the  $(n+1)^{\text{th}}$  point is plotted as a function of the preceding  $n^{\text{th}}$  point is called a return map (e.g., Lorenz, 1963; Kapitaniak and Bishop, 1999). For example, during the analysis of the anisotropy

parameter  $P$  (degree of anisotropy), the first component ( $n$ ) is the oldest data  $P_n$ . The second ( $n+1$ ) in the series is  $P_{n+1}$ , which is younger than  $P_n$ . The third component is  $P_{n+2}$  and so on. The last component is  $P_{n+i}$ , which is the youngest in the series. The first data plotted in the return map is  $P_{n+1}$  in the function of  $P_n$ , the second is  $P_{n+2}$  in the function of  $P_{n+1}$  and so on to the last one, which is  $P_{n+i}$  plotted in the function of  $P_{(n+i)-1}$ . The distribution of the points on the map indicates the frequency of the data in a series (Section 5).

Density maps can be used for the visualization of the return maps. In a density map, areas with various colours or tones indicate the most frequent data in the sequence. The alignment of the data along an axis from the origin ( $x_0, y_0$ ) towards the maximum of the plot ( $x_{max}, y_{max}$  coordinates) shows that the same values appear in the same frequency in the sequence of the data. The random appearance of the areas with higher density in the return map indicates the most frequently appearing data in the series.

### 3.3 Rock magnetic characteristics

Rock magnetic experiments related to loess and paleosol successions are already widely discussed and summarized in previous publications such as Liu et al. (2012), Maher (2016) and Maxbauer et al. (2016). In the following section, we summarize the most common rock magnetic methods that have been applied in magnetic fabric studies of loess.

Frequency-dependent magnetic susceptibility is a powerful indicator of very fine grain, superparamagnetic components. Although it is one of the most commonly applied rock magnetic methods in loess research, it is not the most frequent in magnetic fabric studies (five studies out of approximately 20) as a supporting rock magnetic method. The studies using  $\chi_{fd}$  (e.g., Matasova et al. 2001; Zhu et al. 2004; Bradák et al. 2011; 2018b, Böskén et al. 2019) do not exclusively focus on the magnetic fabric but rather complex environment reconstruction, which involves various methods that are not limited to magnetic methods.

Based on the analysis of magnetic parameters, such as coercivity of remanence (remanent coercive force;  $H_{cr}$ ), coercivity ( $H_c$ ), saturation remanence ( $M_{rs}$ ) and saturation magnetisation ( $M_s$ ), and on the shape of the hysteresis loop, hysteresis experiments can provide information about the type (ferro, para and diamagnetic), magnetic coercivity and magnetic domain/grain size of the contributors in a sample (e.g., Tauxe et al. 1996; Tauxe, 2010). Hysteresis loops and Day-plot are used in the study of e.g., Lagroix and Banerjee (2002), Zhu et al. (2004), Liu and Sun (2012), Ge et al. (2014), Peng et al. (2015) and Xie et al. (2016). Plotting the  $H_{cr}/H_c$  against the  $M_{rs}/M_s$  ratio reveals the multi-domain, single-domain, superparamagnetic and vortex states (SD+MD mixture or pseudo-single domain in earlier studies) of the magnetic mineral components in the samples (Day et al. 1977; Dunlop, 2002; Roberts et al. 2017). Currently, concerns about the use of the Day plot have been raised, which leads to the application of alternative methods (Roberts et al. 2019). First-order reversal curve (FORC) is an alternative assessment of hysteresis curves and Day plot that was applied to determine magnetic domain characteristics in loess magnetic fabric as reported by Cheng et al. (2019).

The combined use of the two methods to describe the relationships among the basic magnetic susceptibility ( $X_{if}$  and  $X_{fd}$ ) and magnetic coercivity ( $H_{cr}$  and  $H_c$ ) parameters can reveal the mechanism of magnetic enhancement in loess during pedogenesis (Forster and Heller, 1997). In magnetic fabric studies of paleosols, “hysteresis vs. magnetic susceptibility parameter plots” may help to describe primary fabric alteration during pedogenesis (Bradák et al. 2018b).

The change in the magnetization of a given sample in the course of isothermal remanent magnetization (IRM) acquisition experiments indicates the characteristic coercivity of magnetic minerals in the sample. Although numerous loess magnetic fabric studies use IRM acquisition curves to obtain such information (Bradák, 2009; Liu and Sun, 2012; Ge et al. 2014; Taylor and Lagroix, 2015; Peng et al. 2015; Xie et al. 2016; Bradák et al. 2018a; Cheng et al. 2019), other potential techniques are useful in IRM studies, e.g., using unmixing techniques to identify various coercivity components in loess sections (e.g., Spassov et al. 2003; Heslop, 2015).

Temperature variation in magnetic susceptibility ( $kT$ ) is a commonly used thermomagnetic experiment during magnetic fabric research (e.g., Lagroix and Banerjee, 2002; Matasova and Kazinsky, 2004; Zhu et al. 2004; Liu and Sun, 2012; Zeeden et al. 2015 and Bradák et al. 2018a). Changes in magnetic susceptibility during heating and cooling processes indicate decay, transformation of various minerals, and the Curie/Néel temperature ( $T_{C/N}$ ) of magnetic contributors. These key alterations and characteristic points during heating and cooling are indicative of various magnetic minerals.

The magnetic mineral characteristics of loess are strongly influenced by local and regional geological settings, representing the most potential source of the material of loess. Despite these differences, the most common magnetic contributors of loess (and paleosol) fabric include a broad range of magnetic grain sizes of (titano)magnetite, maghemite, goethite and haematite along with various paramagnetic components (e.g., phyllosilicates) (see the cited studies above). Along with the information introduced above, a detailed review containing novel results and theories about the magnetic mineral composition and enhancement of loess can be found in the studies of, e.g., Maher (2011, 2016).

#### 3.4 Case study from Paks – Applied methods

As a case study, we analysed the main paleosol units of the Paks section introduced in Table 1. As it is shown in Supplementary Material, ca. five to ten oriented samples were collected from each horizon of the section at depth intervals  $\sim 10$  cm. No plastic boxes were used for sampling and storage to avoid magnetic fabric deformation during sampling and sample preparation. Magnetic fabric was investigated in 252 cubic specimens of  $2 \times 2 \times 2$  cm (Supplementary Material 1). For the magnetic fabric, we measured magnetic susceptibility at low frequency (LF, 976 Hz) and high frequency (HF, 3,904 Hz) using an MFK1-FA Kappabridge (AGICO) with an automatic rotator, providing raw data to characterize the LF AMS (AMSLF) and HF AMS (AMSHF). The intensities and

directions of the principal susceptibilities were determined by computer analysis (Tensor Addition / Subtraction Toolbox in Anisoft5; AGICO, <https://www.agico.com/text/software/anisoft/anisoft.php>). We excluded the results with F test < 3.48, 95% significance level (Jelinek, 1977). F12 (F12 > 5) and e12 parameters (Lagroix and Banerjee, 2004a) were examined along with the alignment of the principal susceptibilities on stereoplots. Lagroix and Banerjee (2004a) and Zhu et al. (2004) summarized the criteria for selecting fabric data with a well-defined orientation (statistically significant  $\kappa_{\max}$ ) for individual loess samples. An area of uncertainty around the orientation of the principal axes was quantified by 95% confidence ellipses with semi-axes, denoted herein by epsilon ( $\epsilon$ ). At the specimen level, the 95% confidence uncertainty ellipse of  $\kappa_{\max}$  is defined by semi-axes  $\epsilon_{12}$  and  $\epsilon_{13}$ , where  $\epsilon_{12}$  is the half-angle uncertainty of  $\kappa_{\max}$  in the plane joining  $\kappa_{\max}$  and  $\kappa_{\text{int}}$  and  $\epsilon_{13}$  is the half-angle uncertainty of  $\kappa_{\max}$  in the plane joining  $\kappa_{\max}$  and  $\kappa_{\text{min}}$ . The maximum allowable  $\epsilon_{12}$  with statistical significance, indicating well-oriented grains in individual samples, is 22.58° (Lagroix and Banerjee, 2004a). Following the application of the criterion, suggested by Lagroix and Banerjee (2004a) and Zhu et al. (2004), only 124 samples out of the 252 measured samples could be used to magnetic fabric analysis.

We used commonly applied AMS parameters, introduced in Table 2, to characterize the magnetic fabric. In addition, we also applied WSA and return map analysis to demonstrate the efficiency of the suggested methods in the analysis of the magnetic fabric of loess.

In addition of AMS analysis, new  $\chi_{fd(fs)}$  results are also presented in the manuscript. To determine the  $\chi_{fd}$ , the susceptibility of the Paks samples was measured at low (0.5 kHz) and high (17 kHz) frequencies (SM 100 portable susceptibility meter, ZH-Instrument, Czech Republic). Absolute ( $X_{fd}$ ) and relative frequency dependence of magnetic susceptibility ( $X_{fd\%}$ ) have been used in environmental magnetic studies (e.g., Dearing et al. 1996). The former can be defined by the following simple equation:

$$X_{fd} = X_{lf} - X_{hf} \quad (\text{Eq. 7})$$

where  $X_{lf}$  and  $X_{hf}$  are the susceptibilities measured at low and high frequencies, respectively. Here,  $X_{fd}$  seems to be strongly dependent on the operating frequency and absolute susceptibility values; therefore, Hrouda (2011, Eq. 13 in the referred study) proposed to use the parameter  $X_{fd}$  (in Hrouda, 2011 it is called  $X_{FV}$ , Eq. 2) normalized by the differences of the natural logarithms of the applied high and low frequencies:

$$X_{fs} = (X_{lf} - X_{hf}) / (\ln f_{hf} - \ln f_{lf}) \quad (\text{Eq. 8})$$

where  $X_{fs}$  is the normalized  $X_{fd}$ , and  $f_{lf}$  and  $f_{hf}$  are the low and high frequencies used during the experiments, respectively.

There are some older measurements from Hungarian loess, also appears in the study and the raw susceptibility data and AMS parameters can be found in Supplementary Material 1. Detailed information about the measurements of those samples can be found in Bradák and Kovács (2014) and Bradák et al. (2018).

#### 4. Formation and alteration of the magnetic fabric of loess

Numerous processes alter the primary magnetic fabric of loess, which is formed during the deposition of dust and the diagenesis of loess. As noted below, the influence of such processes must be considered during magnetic anisotropy studies of loess successions.

##### 4.1 The deposition of dust and diagenesis of loess

There has been a long-standing argument about the ability to record orientation during loess deposition from air. The lack of anisotropic character is probably due to the expected relatively calm environment, which favours the deposition of fine grain dust. Simply put, higher current (wind) energy, which may be able to form oriented fabric, keeps the fine, silt size grains moving. Matasova et al. (2001, p. 377) provided an explanation for the magnetic fabric found in Bachat loess (Siberia): “in the case of aeolian loess deposits wind is the main factor controlling the sedimentation process. However, usually it cannot give strong alignment of dust material because of the significantly lower viscosity of air, compared to water”.

According to Derbyshire et al. (1988), the fabric of the ‘typical’ (i.e., aeolian) loess is isotropic, and every observed anisotropy in loess is developed by post-depositional processes. The theory about the poorly lineated, mainly foliated aeolian loess with insignificant anisotropy is supported by studies of Hus (2003) and Wang and Løvlie (2010). Hus (2003) suggests that gravitational force and vertical compaction play important roles in developing the magnetic fabric of loess. The aim of the experiments executed by Wang and Løvlie’s (2010) was not the characterization of the magnetic fabric; they also simulated the sedimentation of loess by dry deposition and wetting the deposited material. Along with other results they reported that the magnetic fabric (e.g., stereoplot analysis) is a poorly lineated, mainly foliated fabric (Figure 2 in Wang and Løvlie, 2010, p. 397). The isotropic loess fabric theory is also supported by Liu and Sun (2012). These researchers did not identify any preferred fabric orientation, a random distribution was observed in the magnetic fabric of Luochuan loess. The isotropic magnetic fabric is often excluded from analysis; unfortunately, there are only a few studies that report the number of excluded samples compared to the anisotropic samples. In Alaskan loess successions (Lagroix and Banerjee, 2004a), 8% of the 864 pieces of the studied sample and 45% of the 1372 pieces of the studied samples were proven to be isotropic.

In contrast to the isotropic fabric theory, many characteristics of flow-aligned fabric (Section 3; Fig. 5b) can be identified in most loess profiles. The poorly or better clustered orientation of elongated grains distributed along the magnetic foliation plane defines the current orientation

(mainly the orientation of deposition). This magnetic fabric type is the most common in loess deposits and can be used for estimating prevailing wind directions (e.g., Begét et al. 1990; Thistlewood and Sun, 1991; Sun et al. 1995; Wu et al. 1998; Lagroix and Banerjee, 2002, 2004a; Nawrocki et al. 2006; Bradák, 2009; Ge et al. 2014; Peng et al. 2015; Xie et al. 2016).

#### 4.1.1 Sedimentation models and the primary loess fabric

Given the possibility that the deposited dust does not show any anisotropic character, the question arises regarding that circumstances during sedimentation strengthen the anisotropic character of loess so they are able to record the prevailing wind directions. Although the description of magnetic fabric development during deposition (and diagenesis) is essential (and may provide connection between the isotropic and anisotropic aeolian loess theories), studies solving such problems are limited.

Based on the study of loess from successions in Eurasia, Hus (2003) suggested that the magnetic fabric of aeolian loess is influenced by various processes, such as wetting-drying, freezing-thawing and compaction, before and during the diagenesis. Although further changes after burial are likely minimal, the distribution of magnetic lineation ( $\kappa_{\max}$  axes) is random in aeolian loess. Although the study strongly supports the isotropic loess theory, it also refers to some cases from the Chinese Loess Plateau wherein the magnetic lineation may indicate paleowind directions. Such lineation was not only observed in samples from the CLP, specifically from the Alaskan loess. Lagroix and Banerjee (2002) defined the primary aeolian material based on its horizontally foliated magnetic fabric and well-defined magnetic lineation in the foliation plane, which correspond to the direction of sediment transport and deposition. Following such observations, no detailed explanation has been provided regarding the factors and processes that may fix or destroy the primary aeolian magnetic fabric, thereby generating isotropic or anisotropic characteristics.

Some studies reported the relationship between magnetic fabric parameters (e.g., F and P) and grain size characteristics of the studied samples (e.g., Zhu et al. 2004; Liu and Sun, 2012). The grain

size dependence of magnetic foliation may be related to the gravitational force, which possibly aligns coarser grains within the foliation plane more efficiently than smaller grains (Zhu et al. 2004). This finding suggests a relationship between the intensity of the transport medium (i.e., the winter monsoon, which is indicated by the grains size of loess) and the magnetic foliation (i.e., larger grain size results in larger foliation). Along with the intensity of transport energy, compaction is mentioned as an important factor during diagenesis that can rotate the long axes of (magnetic) minerals into the bedding plane and increase the foliation of the material (along with the density) (Zhu et al. 2004).

The model proposed by Zhu et al. (2004) assumed that cold and dry winter monsoons were responsible for the development of the magnetic fabric, but no consensus has been reported about the role of winter and summer monsoons in the formation of imbrication. Zhang et al. (2010) observed the lack of imbricated fabric in loess and proposed a model that emphasizes the importance of precipitation (rain) in magnetic fabric development during the summer monsoon period in China. Based on their theory, the rain “helps to settle the sedimentary and magnetic grains” (Zhang et al. 2010, p. 443) during the summer monsoon period, yielding quasi-horizontal, non-imbricated fabric. The influence of post depositional factors, such as precipitation and vegetation appear, in the model proposed by Ge et al. (2014). In this model, following deposition, the dust particles (including the magnetic grains) are oriented by the surface wind. When the grains are buried, they are immobilized. The study reveals the “aid” of precipitation and vegetation in fixing the grains, but no detailed description is provided. The study only describes the possible disturbing influence of dense vegetation (grains are intercepted before deposition) and water-lain processes triggered by intense precipitation (e.g., sheet-wash, run off water) (Ge et al. 2014).

Revealing additional information about the depositional speed (grain size-dependent factor), magnetic parameters and the distribution of the orientation of principal axes (magnetic fabric types) led to the development of a complex sedimentation model. Bradák et al. (2018a) reported a clear connection between the increasing depositional velocity and the change in magnetic fabric from

flow-aligned to flow-transverse fabric (Fig. 5b, c, d and f), indicating the mobilization of grains during transportation (along with imbrication). In addition, an additional process is proposed, namely, the re-alignment of finer grains on the surface in the direction of prevailing wind before compaction and diagenesis. Such a process may describe the enhancement of the originally random distribution of grains and the formation of weak magnetic lineation. Thus, this model builds a bridge between the isotropic and anisotropic loess fabric theories (Bradák et al. 2018a).

As an alternative solution to identify fabric orientation, Nawrocki et al. (2006) used the orientation of imbrication (i.e., the discrepancy of  $\kappa_{\min}$  axes from the vertical and their alignment on the stereoplot) to determine characteristic wind direction (Fig. 5c). Nawrocki et al. (2006) also suggest that wind strength affects the magnetic fabric. Specifically, lower wind energy forms the flow-aligned magnetic fabric, and stronger winds form the flow-transverse fabric (Fig. 5b and f). This statement was later supported by the quantitative analysis of Bradák et al. (2018a) (see above). In recent work, Nawrocki et al. (2019) (re-)emphasizes the use of imbrication as an indicator of paleowind direction. Based on their observations, imbrication in loess can be identified by comparing the resistant magnetic foliation structure (formed by imbricated platy minerals) with relatively large surface adhesion with weak magnetic lineation (formed by the elongated grains).

As demonstrated by the introduced models, there is no consensus about the “ideal” sedimentation and magnetic fabric-forming model, which may change from site to site. Moreover, sedimentation is strongly influenced by post-depositional processes, which alter the primary (aeolian) fabric of loess.

#### 4.2 Case study from Paks – Effect of reworking and pedogenesis

Soil formation (pedogenesis) is expected to alter the primary fabric by reworking processes, mineral alterations, and neoformation processes. The former (reworking) involves physical processes and the reorientation of magnetic components by, e.g., roots and burrows, which are formed by

biogenic activity (bioturbation). The latter is related to chemical alterations triggered by, e.g., weathering and bacterial activity.

#### 4.2.1 Alteration of the primary fabrics by physical disturbances during pedogenesis

As a possible indicator of physical disturbance of horizontally oriented grains by reworking (bioturbation), a chaotic and/or vertically oriented magnetic fabric is expected to be found in paleosols intercalated in loess layers. Matasova et al. (2001) and Matasova and Kazansky (2004) observed chaotic and vertically oriented magnetic fabric in paleosols of Siberian loess profiles. Along with the disturbed and reoriented magnetic fabric, a well-preserved sedimentary fabric is also found in paleosols. The appearance of various fabric types led the authors to conclude that the distribution, e.g., the degree of disturbance compared to the primary sedimentary (flow-aligned) fabric, is a sensitive indicator of the degree of pedogenesis (Matasova and Kazansky, 2004). Matasova and Kazansky (2004) support their theory with the comparison of the AMS degree and the frequency dependence of magnetic susceptibility (data originally published in Jordanova and Jordanova, 1999). The study observed an inverse correlation between the AMS degree and pedogenic intensity. The increased degree of pedogenesis corresponds to reduced preservation of the initial sedimentary fabric of parent loess, which is distorted or lost by pedogenic reworking (Matasova and Kazansky, 2004).

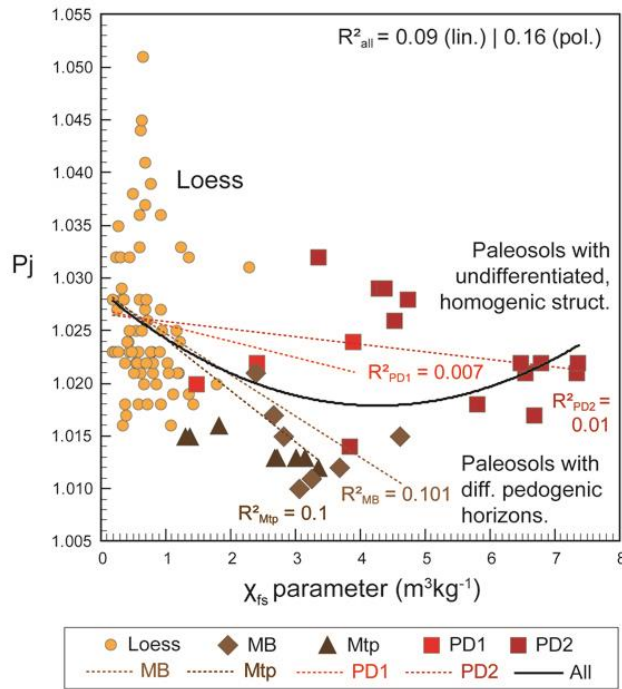


**Figure 6.** The relationship between the alteration of the primary fabric and pedogenesis ( $X_{fs}$  – Pj plot). Paleosols with well-differentiated pedogenic horizons are indicated by brown colours, and paleosols with undifferentiated, homogenic structure are indicated by red colours.

To test the relationship between the change of anisotropy degree and the development of paleosols, we elaborated a similar analysis to Matasova and Kazansky (2004) using  $f_{Pj}$  (Eqn. 3) and  $X_{fs}$  (Eqn. 8) parameters of sediment and paleosol units of Paks loess succession (Suppl. Mat. 1; Fig. 6). The analysis of  $X_{fs}$  and  $f_{Pj}$  plots reveals a somewhat more complex relationship between the alteration of magnetic fabric and the degree of pedogenesis in paleosols. As shown in Fig. 6, the expected inverse linear relationship is not evident in Paks succession ( $R^2=0.09$ ), but a minimal tendency is demonstrated by the polynomial trend ( $R^2=0.16$ ). The tendency depicted by the trends separately applied on the studied units suggests that the observation of Matasova and Kazinsky (2004) can be applied in the case of MB and Mtp paleosols, wherein the  $X_{fs}$  – Pj plot exhibits a weak inverse relationship (for both,  $R^2 \approx 0.1$ ; Fig. 6). Such an inverse relationship (any significant relationship) cannot be identified in PD1 and PD2 paleosols ( $R^2 \approx 0.01$ ; Fig. 6). The differences in pedogenic characteristics of the studied soils may describe the differences that appeared on the  $X_{fs}$

and  $P_j$  plots. The well-separated soil subhorizons of MB and Mtp (e.g., E – eluviated and B – clay accumulation horizon) indicate intense vertical differentiation in the body of the soil. This differentiation can be caused by various processes (e.g., leaching, vertical pore water migration and material movement), and these processes can disturb the original sedimentary fabric during the development of the soil as well. Such subhorizons do not appear in the PD1 and PD2 units, the paleosols of which are characterized by massive, homogeneous structures. Such a homogeneous structure (along with increasing compaction) may prevent the alteration of the original sedimentary fabric (Bradák et al. 2018b). Although this theory may be applied to paleosols, more AMS measurements are needed to obtain convincing information about the relationship between frequency-dependent magnetic susceptibility and AMS parameters due to the limited number of paleosols samples introduced in Figure 6.

An additional explanation of the absence of negative linear correlation between  $X_{fs}$  and  $P_j$  observed in older paleosols from Paks section (PD1 and PD2 units) is possibly related to the different type of magnetic contributors, dominant in the magnetic fabric. Based on the physical characteristics of the paleosols (homogenic, compact, red coloured horizons; Table 1) and their possible forming environment (defined as “Mediterranean forest soil” in some studies) PD1 and PD2 contain higher amount of hematite (possibly in SP fraction, as the result of pedogenic processes). The sub-fabric formed by hematite may differ from the AMS and altering the  $P_j$  values, while the high  $X_{fs}$  indicates the SP hematite fraction (e.g. Wells et al. 1999). To verify this theory more magnetic measurements are needed.

The results from Paks suggest that the type of paleosols and the processes that are represented by the soil types are significant factors in the alteration and preservation of sedimentary fabric. This theory is supported by various studies. Bradák et al. (2011) and Bradák-Hayashi et al. (2016) report that the well-developed paleosol, which are characterized by differentiated pedogenic characteristics and low anisotropy degrees (similar to MB and Mtp from Paks), did not show a chaotic grain orientation but a well-aligned vertically oriented fabric. Vertical grain orientation was

interpreted as a result of leaching and vertical migration in the soil body in a relatively humid environment with significant annual precipitation (Bradák-Hayashi et al. 2016).

In the tundra gley horizons of Nussloch loess (Taylor and Lagroix, 2015), the influence of bioturbation (and the appearance of freezing-thawing processes in the upper part of the soil) caused the significant decrease in  $P_j$ . In addition, tundra gley horizons show  $16^{\circ}$ – $30^{\circ}$  dips of their magnetic foliation planes as a possible mark of particle remobilization in stagnating water or percolating water environments (Taylor and Lagroix, 2015). Compared to the tundra gley horizons, the magnetic fabric of arctic brown soils or cambisols of the profile did not show a significant difference compared to the magnetic fabric of their parent material. This finding suggests that they may not have developed into very mature soils possibly due to the limited water availability (Taylor and Lagroix, 2015).

In the study of the composite section of Titel-Stari Slankamen succession (Marković et al. 2011; Buggle et al. 2013, 2014), no significant differences were found in the magnetic fabric parameters of the sedimentary units and differently developed paleosol horizons, suggesting that the pedogenic processes did not alter significantly the magnetic fabric (Song et al. 2018). In contrast, studies from Hungarian loess show (e.g., Bradák et al. 2011) that loess and well developed paleosol horizons are characterized by similar AMS parameters (e.g.,  $F$ ,  $L$ ,  $P_j$  and  $T$ ), but the alignment of the principal susceptibility axes indicate the alteration of the primary magnetic fabric (i.e., changes from a horizontally to vertically oriented fabric).

#### 4.2.2 Mineral neoformation

Along with the physical transformation of the fabric, neoformation of minerals may play a role in the change of the magnetic fabric in paleosols. The “vertical orientation” of the fabric is attributed to the inverse fabric exclusively built by SD magnetite (more information is provided in Section 3), and the influence of pedogenic SP components on the primary sedimentary magnetic fabric is poorly known (Jordanova et al. 1996; Bradák et al. 2018b; Hrouda et al. 2018). Hus (2003) recognized only a

moderate modification of the primary fabric parameters, namely, a slight decrease in P and F, which may indicate that soil magnetic enhancement due to authigenic magnetites only exhibits a minor influence on the overall fabric (Hus 2003; p. 697).

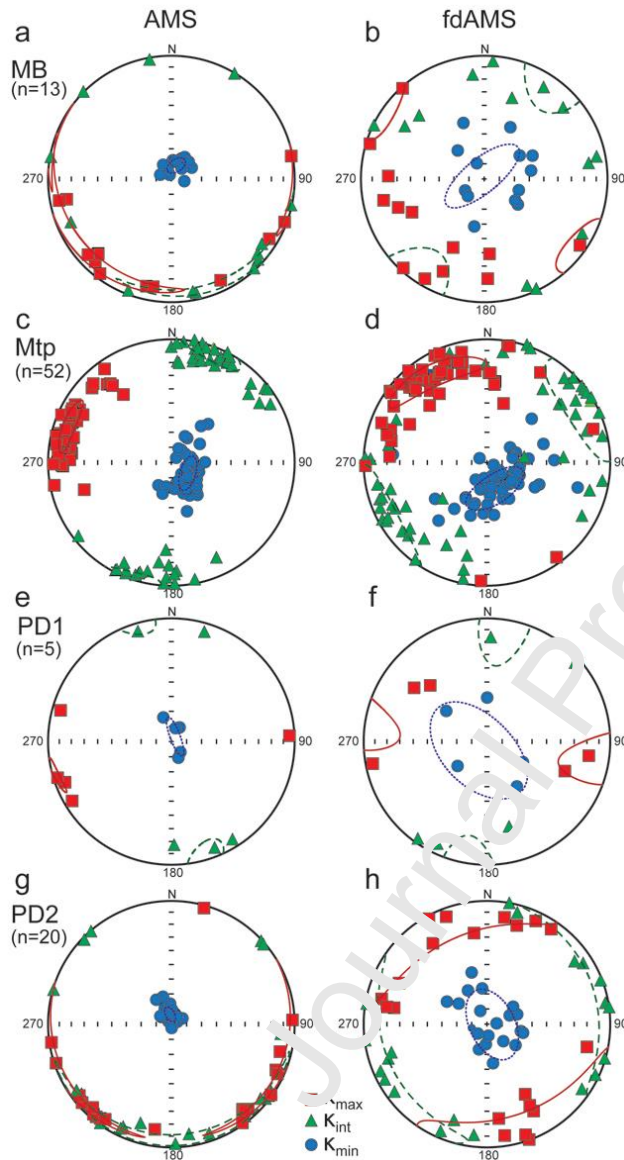


**Figure 7.** Comparison of bulk (AMS) and nanofabric (fdAMS) of paleosols from Paks. The alignment and scattering of the principal susceptibilities are represented by 95 percent confidence ellipsoids, which are indicated by red solid ( $\kappa_{\max}$ ), green dashed ( $\kappa_{\text{int}}$ ) and blue dotted ( $\kappa_{\min}$ ) lines. The principal susceptibilities were plotted on stereoplots using an equal-area projection and geographical coordinate system.

To further assess the influence of mineral neof ormation on the primary magnetic fabric, the nanofabrics of four characteristic paleosol horizons, MB, Mtp, PD1 and PD2, from Paks were characterized by the calculation of fdAMS based on the data reported by Bradák et al. (2018b) (Suppl. Mat. 1; Fig. 7). Compared to AMS results, which indicate generally horizontally oriented magnetic grains for any magnetic grain size and type (Fig. 7a, c, e and g), the nanofabric of the studied paleosols exhibit a more scattered distribution (Fig. 7b, f and h). Only one exception is noted; specifically, the nanofabric of Mtp unit exhibits principal susceptibility orientations with a scattered distribution that seem to follow the alignment of the AMS fabric with a ca. 45° clockwise horizontal shift (Fig. 7d). The random distribution of principal susceptibility axes indicates the random orientation of authigenic SP grains. The results from Paks loess generally verify the observations of Hus (2003), i.e., neof ormed SP magnetic grains have an insignificant influence on the overall fabric in the studied paleosols.

Despite the randomly oriented nanofabrics observed in most of the studied paleosols, the appearance of relatively well-aligned nanofabrics draws attention to pedogenic processes that may form similar alignments as nano-size grains as the primary fabrics. Jordanova et al. (1996) provides a possible explanation for this phenomenon. Based on some analogous observations of recent soils, Jordanova et al. (1996) suggest that the grain shape of the authigenic SP minerals (i.e., the magnetic fabric formed by the SP contributors) would follow the preferred crystallographic orientation of silicates (e.g., montmorillonite) found in paleosols. This theory is supported by Hyodo et al. (2020) who identified fine-grained pedogenic magnetic inclusions in the coarser detrital minerals in loess from the CLP.

#### 4.3 Case study from Paks - Redeposition and higher energy transportation

The magnetic fabric of aeolian loess is generally described as a flow-aligned (oriented) and imbricated fabric (Section 3; Fig. 5b and c), and irregular cases are only reported in few studies. One

of the irregular types is the uncommon flow-transverse (biaxial-prolate, pencil, or AB plane imbricated) fabric (Section 3; Fig. 5e and f), which has been found in four loess successions (Lagroix and Banerjee, 2004b; Bradák et al. 2011; Bradák-Hayashi et al. 2016; Zeeden et al. 2015; Bradák et al. 2018a). The development of such a magnetic fabric is interpreted to result from, e.g., strong currents and the traction and rolling of grains during transportation (e.g., Ellwood, 1979; Ellwood et al. 1979; Ledbetter and Ellwood 1980).

Flow-transverse fabrics are easily identified in loess due to the characteristic and different alignment of the principal susceptibilities on stereoplots compared to regular flow-aligned aeolian fabrics (Fig. 5). Both aeolian (e.g., Bradák et al. 2018a) and water-lain processes (Lagroix and Banerjee, 2004b, Bradák et al. 2011; Bradák-Hayashi et al. 2016) can develop very similar flow-transverse grain alignments in the sedimentary magnetic fabrics; therefore, such processes cannot be distinguished by the distribution of the direction of principal susceptibility axes on stereoplots. A comparison of the AMS parameters of aeolian and water-lain (partly) laminated materials on various plots may help to separate the two groups. To test the hypothesis, various loess samples representing various sedimentary facies were compared, such as: 1) fine grained, partly laminated aeolian material characterized by flow-transverse fabric from Paks (Bradák et al. 2018a); 2) a unit from Cérna Valley with similar sedimentary characteristics but with flow-oriented MF (Bradák et al. 2011); 3) water-lain, laminated material (consisting of alternating loess and paleosol laminae) characterized by flow-transverse fabric (Bradák et al. 2011); and 4) samples from various profiles (Hévízgyörk, Vácbotyán and Verőce) with similar redeposited, laminated material and flow-oriented magnetic fabric (Bradák and Kovács, 2014).

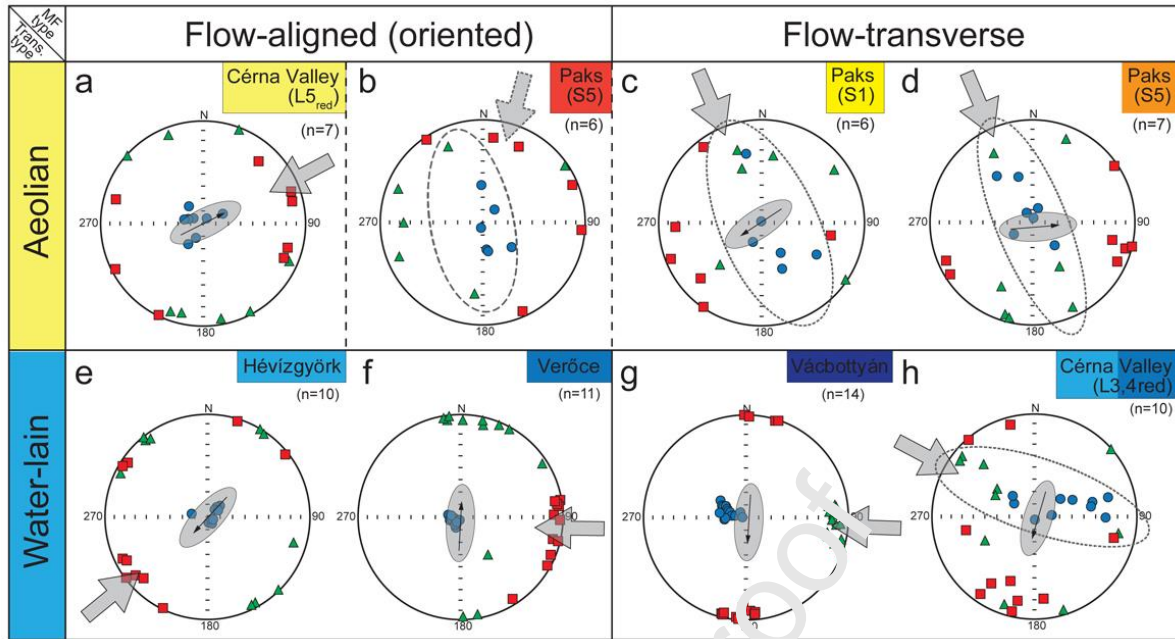


**Figure 8.** Magnetic fabric types from various Hungarian loess successions. a) Poorly oriented flow-aligned aeolian fabric from fine laminated loess; b) flow-aligned/flow-oblique aeolian fabric from partly laminated sandy loess; c) and d) flow-transverse (Type 2; Fig. 5f) aeolian fabric from (partly) laminated sandy loess; e) poorly oriented flow-aligned water-lain fabric from laminated redeposited loess; f) well oriented flow-aligned water-lain fabric from laminated redeposited loess; g) flow-transverse (Type 1; Fig. 5e) water-lain fabric from laminated redeposited loess; and h) flow-transverse (Type 2; Fig. 5f) water-lain fabric from laminated redeposited loess. The areas marked by dotted lines (Fig. 8c, d, and g, h) indicate the intermixing of principal susceptibilities in flow-transverse magnetic fabric (Sub-section 3.2.4). The grey arrows and the grains with small black arrows indicate the relationship of paleocurrents and the alignment of grains with preferred dimensional orientations, respectively. The area marked by a dashed line (Fig. 8b) indicates the plunge of foliation plane (discrepancy of  $\kappa_{\min}$  from the vertical), which is a potential mark of the transformation of magnetic fabric from flow-aligned to flow-transverse (e.g., Bradák et al. 2018a). Note that the same background colour coding of sampling site names is also used in Fig. 9.

As shown in Figure 8, the MF of the chosen sediments can be characterized by flow-aligned (Fig. 8a,[b], e and f) and flow-transverse (Fig. 8c, d, g and h) characteristics for magnetic fabrics formed by aeolian (Fig. 8a, b, c and d) or water-lain processes (Fig. 8e, f, g and h). The relationship between the degree of foliation ( $F$ , Eq. 1) and degree of lineation ( $L$ , Eq. 2) was plotted in the Flinn diagram (Fig. 9a). The change of anisotropy degree ( $P_j$ , Eq. 3) and the shape of susceptibility ellipsoid ( $T$ , Eq. 5) due to the possible influence of various transport agents were investigated using the Jelinek plot (Fig. 9b). The connection between magnetic fabric parameters  $q$  (Eq. 6) and  $\beta$  and the sedimentary environment was studied using Taira plots (Fig. 9c and d). As shown in Figure 9, the samples from various loess types (i.e., aeolian and water-lain) are intermixed in the Flinn, Jelinek and in the Taira plots. The attempt to separate the flow-transverse fabric developed by aeolian or water-lain processes failed, and the separation of magnetic fabric (partly) related to various transport agents or sedimentary environments was not possible.

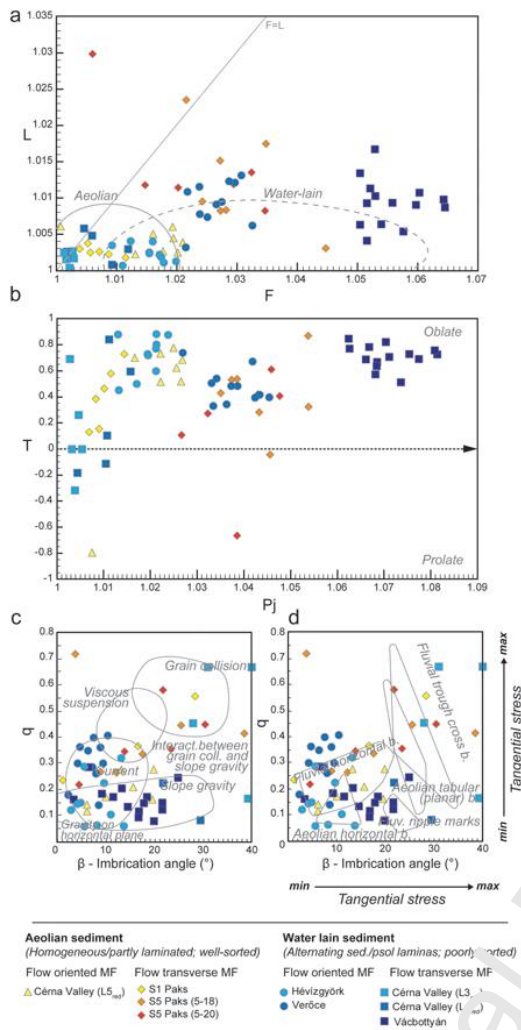


**Figure 9.** Separation of the laminated aeolian and water-lain redeposited loess magnetic fabric based on their AMS parameters (magnetic fabric types introduced in Figure 7). a) F-L (Flinn) plot with the areas defining aeolian (dotted line) and water-lain (dashed line) loess proposed by Liu et al. (1988); b) Pj-T (Jelinek) diagram; c and d)  $\beta$ -q (Taira) plot (Section 3). The various locations marked by grey polygons in Figure 8 c and d indicate various characteristics of transport medium (c), and the type of sedimentary structures (d) determined by the  $\beta$  and q values of sediments in Taira (1989).

#### 4.4 Post depositional compaction, deformation and other processes

Among the processes that may alter the original sedimentary fabric, compaction may influence the units of a loess/paleosol sequence continuously after deposition, which is triggered by the burial

and unloading of additional materials. Zhu et al. (2004) and Bradák et al. (2018) observed increasing degrees of foliation by depth as a possible result of post depositional compaction, which rotates the long-axes of magnetic minerals ( $\kappa_{\max}$ ) into the bedding plane. Liu and Sun (2012) reported similar tendencies in the degree of anisotropy. Matasova and Kazansky (2004) suggest that the “high AMS degree, preferred orientation of AMS axes and essentially oblate magnetic fabric testify that these loess layers have undergone compaction only, without any secondary reworking” (Matasova and Kazansky, 2004, p. 169).

A more significant indication of deformation by a stress field is noted by the development of the so-called biaxial prolate ( $\kappa_{\max} > \kappa_{\text{int}} \approx \kappa_{\min}$ ) or biaxial oblate magnetic fabrics ( $\kappa_{\max} \approx \kappa_{\text{int}} > \kappa_{\min}$ ) (Lagroix and Banerjee, 2004b). Compared to the flow-transverse-like biaxial prolate magnetic fabric, the directions of  $\kappa_{\min}$  axes are well clustered in the biaxial oblate fabric, and the  $\kappa_{\min}$  and  $\kappa_{\text{int}}$  axes create a girdle perpendicular to the  $\kappa_{\min}$  axis.

Such deformation-related fabric types are rare and have been reported only from Gold Hill Steps loess (Alaska; Lagroix and Banerjee, 2004b) and Paks loess succession (ELB; Bradák et al. 2019a). In the former case (Gold Hill Steps, Alaska), the sequence of orientation distributions is “consistent with deformations associated with permafrost degradation during periods of climate amelioration” (Lagroix and Banerjee, 2004b, p. 456). The biaxial prolate orientation resulted from shear stress, and the lateral translation of the units below the deformed sections are possibly related to permafrost activity. A biaxial oblate fabric may form when the material behaved as rigid bodies in a permafrost state. Based on the observed macroscopic features and the magnetic fabric parameters, Lagroix and Banerjee (2004b) built a model that describes the section as a complex permafrost system, and the magnetic fabric are formed by various factors, such as the behaviour of active and impermeable layers and the channelling flow of groundwater.

In the latter case (Paks, ELB), the biaxial oblate fabric was interpreted as the result of 1) sin- or post-depositional horizontal strain (i.e., compression); 2) water-saturated high-density flow; 3) water saturation and later-stage deformation of the primary fabric associated with the slow emplacement

of the material (i.e., the development of rheomorphic magnetic fabric by creeping); and 4) (theoretical) stable single domain magnetic fabric (Bradák et al. 2019a).

#### 4.5 Sub-fabrics of loess

As it is already described in Sub-section 3.1, AMS measurements reflect the orientation of all grains in the material, including superparamagnetic, paramagnetic, ferri and antiferromagnetic contributors. Such contributors form sub-fabrics in loess which may provide much reliable information about the formation and alteration of the magnetic fabric of loess. Unfortunately, there is only a few studies, which focuses on sub-fabrics in loess.

Aeolian, primary loess is characterized by low magnetic susceptibility which may suggest that paramagnetic components contribute significantly to the bulk magnetic susceptibility value (Rochette, 1987; Hrouda and Jelinek, 1990). The significance of paramagnetic contributors in the magnetic fabric of loess were suggested by e.g. Hus (2003), Taylor and Lagroix (2015) and Bradák et al. (2018). The study of the relationship between the mean magnetic susceptibility and anisotropy degree may help to reveal the influence of paramagnetic contributors, i.e. in the case of the dominance of paramagnetic sub-fabric no relationship can be recognized between the two parameters (Hus, 2003; Taylor and Lagroix, 2015).

During the study of loess magnetic fabric, numerous samples are characterized by strongly oblate fabric which may indicate paramagnetic sub-fabric carried by minerals such as biotite and muscovite (Martín-Hernández and Hirt, 2003; Bradák et al. 2018a). As it was suggested by Bradák et al. (2018), phyllosilicates may be capable of weakening the anisotropy of the magnetic fabric. Moreover, due to their oblate fabric symmetry,  $k_{max}$  and  $k_{int}$  axes of phyllosilicate-dominated fabric are poorly or randomly aligned (Biedermann et al. 2014).

Antiferromagnetic contributors, especially e.g. hematite is common in loess and paleosol successions as well. It may appear in the sediment as the detrital remain from the source area (e.g. Paks, European Loess Belt) of the deposit but also can form under certain climatic condition (e.g. CLP).

Despite the numerous publications related to hematite in loess, the hematite sub-fabric of loess is poorly known. Jordanova et al. (1996) identified SD or near SD states and multidomain (MD) magnetite and hematite grains in the fabric of Bulgarian loess by the application of anisotropy of isothermal remanent magnetization. Besides this study, there has not been any other study which focus on antiferromagnetic (hematite) sub-fabric of loess.

As it is already discussed in Sub-section 4.2 pedogenic processes may increase the amount of superparamagnetic contributors and form superparamagnetic sub-fabric. Besides the suggested studies above (Bradák et al. 2018b; Hrouda et al. 2018), no other study have been elaborated on loess and paleosol sections yet, although the analysis of superparamagnetic sub-fabric in paleosols may provide insight of pedogenic processes and bacterial activity in the body of the soil.

Despite the small number of studies focused on the sub-fabrics in loess, there has been increasing number of research dealing with the identification and separation of sub-fabrics of para-, dia-ferro-, antiferro- magnetic components in a composite media (various type of rocks, sediments and so on) (e.g. Martin-Hernandez and Hirt, 2003; Martin-Hernandez and Ferre 2007). The analysis of different statistical methods applied for calculation of AMS ellipsoid may also provide useful information about the sub-fabrics, existing in the studied material (e.g. Guerrero-Suarez and Martin-Hernandez, 2014).

## 5. Discussion - Significance of magnetic fabrics in environmental reconstruction

### 5.1 The ultimate goal – the Reconstruction of paleowind direction

Can prevailing wind directions be identified by the analysis of the magnetic fabric of aeolian loess? This question has been asked since the beginning of magnetic fabric studies, and the answer seems to be more complex than might be expected (Fig. 10 and Suppl. Mat. 1).

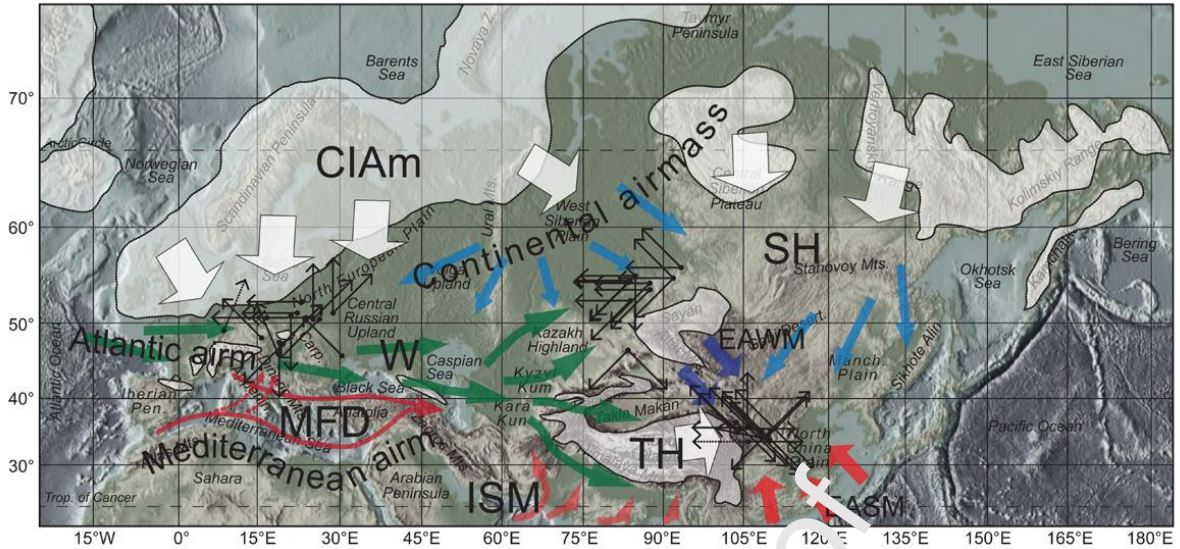


**Figure 10.** Prevailing wind directions identified in the Eurasian loess successions during the Pleistocene. The black arrows indicate profiles with reconstructed wind directions. The coloured arrows indicate characteristic winds, such as air masses appearing over Eurasia: green – Westerlies (W) and Atlantic air masses. The red arrow over the Mediterranean indicated the Mediterranean Front Depression (MFD) and Mediterranean air masses. The red arrows over India indicate the Indian Summer Monsoon (ISM). The red, wide arrows over East Asia indicate East Asian Summer Monsoon (EASM). Light blue arrows indicate Siberian High (SH) and continental air masses; white arrows indicate “katabatic” winds from continental and mountain ice sheets, which potentially formed due to the quasi-permanent high-pressure air masses over the ice sheets, such as Tibetan High (TH) and continental ice sheet air mass (CIAM). The maximum spread of continental ice sheet and mountain glaciation is marked by white polygons based on the Last Glacial Maximum data from Scotese (2013) and Batchelor et al. (2019). The basic relief map is adapted from Amante and Eakins (2009). The list of the profiles (including references) used in the map can be found in Supplementary Material 1.

Based on the studied sections and their geographical location, the loess successions represent various regions and timeframes from the Pleistocene. Such complex results identified in various successions are influenced by numerous factors, and may indicate various climatic and/or

environmental components. As it is shown in the previous section (Sub-section 4.2), there are many factors controlled by the regional climate/environmental regime which may alter the magnetic fabric. In this section, we focus on the loess-paleosol sections for which it was possible to reconstruct some prevailing wind direction. More information about the alteration of the primary aeolian fabric can be found in Sub-section 4.2.

#### 5.1.1 Characterization of the rhythm of East Asian monsoon

A couple of studies, which were mainly performed during the first period of research on the AMS of Chinese loess (e.g., Huang and Sun, 2005; Liu et al. 2008; Sun et al. 1995; Thistlewood and Sun, 1991; Wang et al. 1995; Zhong et al. 1996), showed a NW–SE fabric orientation. The identified NW orientation was interpreted as a direction of winter monsoons that primarily flow from the central Asian desert areas and determine the grain orientation not only in loess but also paleosol horizons (Ge et al. 2014) (EAWM, Fig. 10).

Among such early studies, some doubt was raised about the NW-SE winter monsoon theory given the results of Zhu et al. (2004), who reported complex fabric orientation corresponding “to dust carried by the NE winter monsoon and moisture transported by the SE summer monsoon” (in Zhang et al. 2010, p. 437). The reconstruction of the summer monsoon routes indicates a SE to NW prevailing direction in the study of Zhang et al. (2010), and the unusual NE direction was interpreted as local disturbance triggered by the corridor between north and south Liupan Mountains. Referring to the observation of Zhu et al. (2004), Liu et al. (2008) suggests no significant change in the wind direction during the Early Pleistocene, but a significant change is noted in the Late Quaternary (Fig. 10).

In 2010, it was established that the magnetic fabric of (Chinese) loess preserved the prevailing wind direction and can be used as a paleoclimate proxy. In that period, Liu and Sun (2012) reported the detailed magnetic fabric study of Louchuan loess with an unexpected twist: “magnetic lineations show no preferred directions and thus cannot indicate paleowind patterns” (Liu and Sun, 2012; p.

488). Liu and Sun suggest that the lack of preferred lineation (i.e. the direction of prevailing wind direction) is possibly caused by multiple factors, such as particle size, pedogenesis, and compaction.

Despite the results of Liu and Sun (2012), more recent studies describe an increasing number of factors influencing the development of wind pattern over the Chinese loess in the Pleistocene. Ge et al. (2014) reconstructed three different characteristic wind directions from the Late Pleistocene (NW–SE at Xifeng, Baicaoyuan, and Yichuan; NE–SW at Lingtai; and E–W at Wudu and Lanzhou) and suggested that the orientation of the magnetic fabric is formed mainly by the patterns of regional surface wind rather than the pattern of large-scale atmospheric circulation (Ge et al. 2014) (Fig. 10).

Along with, e.g., focusing on long-term climate trends (e.g. aridification) and its influence on the circulation pattern (Xie et al. 2016), tectonic processes, i.e., the uplift of the Tibetan Plateau, are also taken into account in the development of characteristic wind patterns (Peng et al. 2015). Such topographical change triggers glacial anticyclone formation over mountains with glacial accumulation regions and interferes with the pattern and characters of Westerlies and the Siberian High (Cheng et al. 2019) (e.g., TH; Fig. 10).

As the results show, there is a significant change in the characteristics of the magnetic fabric developed in various part of the CLP. Such differences are influenced by various environmental factors which may e.g. i) affect the prevailing wind direction (e.g. topographical characteristics), and ii) alternate the primary magnetic fabric and make the identification of dominant wind direction impossible (e.g. increasing precipitation from Western regions toward East).

#### 5.1.2 Characterization of wind regimes in Siberia, Europe and Alaska

The present day climate-subzones of Siberia along with the seasonal change in wind direction are reflected in the magnetic fabric parameters (Matasova and Kazansky, 2004). The stable W-E to SW-NE, WSW-NNE (aeolian loess in general) to W-E (MIS2 loess unit in general) and SW-NE to S-N (Lozhok and Mramorny) wind directions suggests that the main climate characteristics have not

changed since the late Middle Pleistocene (since 180 ka); only the amplitude of the climate fluctuations is different.

Among many climatic factors, including the influence of various climate centres, the permanent cold air masses over the growing continental ice sheet might play one of the most significant roles in the wind system over Europe during the glacial periods (Fig. 10). West and southwest prevailing wind directions were revealed in Poland and western Ukraine (North European Plain) following the strike of the Late Pleistocene (Weichselian – MIS2) ice sheet margin and parallel to the axis of the lowland located between the ice sheet and the Carpathians and Podolian Upland (Fig. 10; Nawrocki et al. 2006). Later, studies from the region indicate a more complex system. The vertical change in the magnetic fabric parameters identified in loess successions from Ukraine indicates the fluctuation of the ice sheet during the Late Pleistocene (Nawrocki et al. 2019). Stable, northern and northeastern katabatic wind developed as the Last Glacial Maximum ice sheet advanced. The appearance of southwestern and southeastern chaotic wind regimes interrupting katabatic wind periods can be interpreted as an indicator of fluctuations in the advancement of the ice sheet. Compared to the clear influence of the ice sheet identified in Poland and Northern Ukraine, the NW wind observed in Southern Ukraine (Roxolany loess) indicates the same direction as the present-day summer wind. The joint AMS and U-Pb isotopic study of loess suggests that the material of loess originated from the Carpathian and Podolian source area, was transported by the Dniester River and redeposited by wind from its sediments (Nawrocki et al. 2018).

Similar to that noted in Southern Ukraine, a similarity exists between the characteristic NW and NE wind directions of the late Middle Pleistocene and present-day wind directions in the northern part of Middle Danube basin (Bradák 2009). Such wind directions indicate the influence of Westerlies and Continental air masses, respectively. In the same region (Central Europe), the dominance of western winds was identified in Moravia (Czech; Obersteinová, 2016) and Krems-Wachtberg (Austria; Zeeden et al. 2015) during the Late Pleistocene, supporting the notion of the influence of Westerlies in the area (Fig. 10).

Although the results from Nussloch loess (Germany; Taylor and Lacroix 2015) are considered to be highly speculative due to the low concentration of magnetic minerals, the NNE-SSW direction may indicate the influence of the continental ice sheet in the western part of the European Loess Belt.

The characteristic shift from the NW-SE to N-S direction during glacial and interglacial periods was identified in Alaskan loess (Lacroix and Banerjee 2002). In a latter work, the temporal wind directions were interpreted in two ways (Lacroix and Banerjee 2004a). In the first scenario, changes in paleowind direction correspond to the substages of MIS5, 5a (warm), 5b (cold), 5c (warm), 5d (cold), and 5e (warm). The second, more appealing scenario connects the periods with various prevailing wind to MIS5, 6 and 7.

Similar to the loess from the CLP, there are many factors which influenced the formation and alteration of the Siberian loess, the loess in European Loess Belt and Alaska. In Siberia, the character of climate components, especially wind, seems to be quasi-permanent: the reconstructed paleowind directions are similar to the present day directions (e.g. Matasova and Kazansky, 2004). Loess successions formed closer to the continental ice sheet directly influenced by the katabatic winds in Europe (katabatic winds, e.g. Nawrocki et al. 2006, 2019) during glacials. In many cases in European loess as well in Alaska, present day wind directions can provide a hypothetical base during the reconstruction of paleowind direction, but the strengthening or weakening of some wind pattern can be observed following the glacial (stadial) and interglacial (interstadial) phases. Along the prevailing wind direction information, the primary magnetic fabric is altered by various processes. In the western part of the European Loess Belt and Alaska the appearance of periglacial and permafrost processes seems to be significant (e.g. Lacroix and Banerjee, 2004b; Taylor and Lacroix 2015). In the Middle Danube Basin (e.g. the Hungarian profiles) intense pedogenic processes have strong influence on the primary aeolian fabric.

## 5.2 The conceptual model for magnetic fabric development in loess

All the processes, forming and altering the magnetic fabric of loess-paleosol successions suggested in Section 4 and Sub-section 5.1, are summarised in a conceptual model (Fig. 11) to demonstrate the complexity of the “responsible” factors.

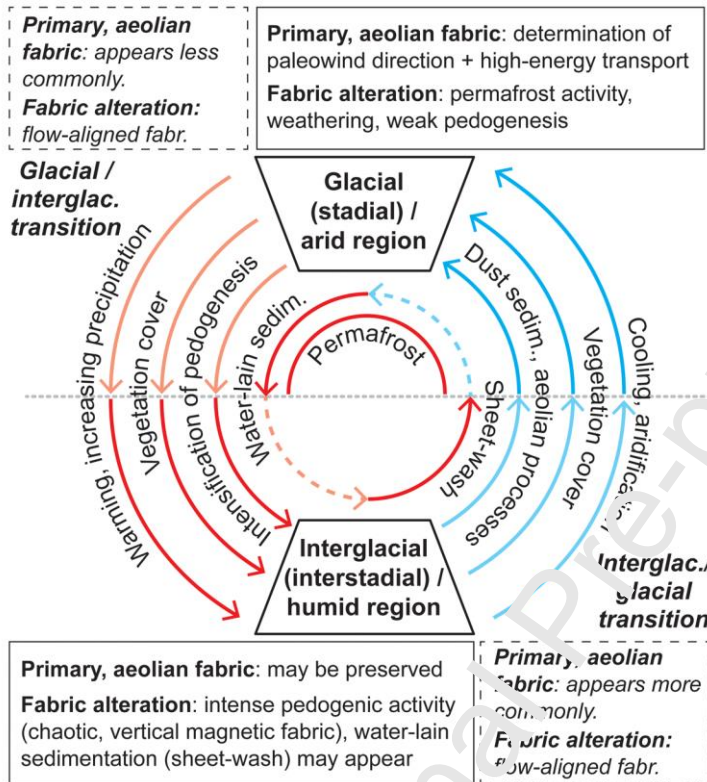


**Figure 11.** A simplified conceptual model to demonstrate the development of magnetic fabric of loess and the complexity of responsible factors. The red arrows indicate the intensification, the blue arrows indicate the weakening of the suggested process. The information in dashed line brackets is about transition periods between glacial and interglacial phases. (Detailed information about the magnetic fabric development can be found in Section 4 and subsection 5.1)

As it is shown in Figure 11, the model summarises the processes which may significantly influence the magnetic fabric development in middle and high latitude loess in the Northern Hemisphere. The model contains three characteristic forming phases: the glacial (stadial)/arid and

interglacial (interstadial)/humid periods, separated by the transition phase. The former (arid) phase is characterized by increasing dust accumulation, sedimentation, the forming of primary, aeolian fabric. The magnetic fabric developed in this period most likely preserves the prevailing wind direction characteristic for aeolian loess units in loess successions from Alaska to the Eurasian loess belts (Fig. 2a). In addition of aeolian sedimentation, the alteration of magnetic fabric may happen due to the increasing permafrost activity (and/or freezing-thawing), most likely in higher latitude regions such as Alaska (Lagroix and Banerjee 2004b), but may appear in middle latitude regions as well e.g. in Nussloch (Taylor and Lagroix, 2015) and Paks (Bradák et al. 2019a).

The low degree of vegetation cover and harsh weather conditions can allow the (re-)mobilization and formation of magnetic fabric, characteristic of high-energy transportation (e.g. duststorms). Flow-transverse fabric in homogeneous or laminated material may indicate such climatic events in Krems-Wachtberg (Zeeden et al. 2015) and Paks (Bradák et al. 2018a) successions.

The other main characteristic phase of magnetic fabric development is the interglacial/humid phase, which is characterized by increasing precipitation and paleosol forming. There is still no consensus about the effect of paleosol forming on the primary fabric. As it is shown by various studies the effect of pedogenesis most likely depend on i) the type and ii) the degree of pedogenesis (Matasova et al. 2001; Matasova and Kazansky 2004; Bradák et al. 2011; Bradák-Hayashi et al. 2016; Taylor and Lagroix, 2015, and Bradák et al. 2018b). Weakly developed weathered horizons and paleosols may not change significantly the primary magnetic fabric, increasing intensity of pedogenic processes may cause the disturbance (chaotic magnetic fabric) or the re-alignment (vertical magnetic fabric) of the magnetic grains. As it has been observed in Paks, no chaotic or vertical fabric can be found in some well-developed paleosol horizon (PD1 and PD2, Table 1, Fig. 6 and 7).

Mineral neoformation must be also considered as an important factor in fabric development during interglacial, but, in present day, there is only a limited number of information about this process (e.g. Jordanova et al. 1996; Hus, 2003; Bradák et al. 2018b; Hrouda et al. 2018).

The transition phase between interglacial and glacial periods can be characterized by decreasing vegetation and still relatively high precipitation. The decreasing vegetation cover together with the appearance of heavy rains (thunderstorms) may lead to intense surface erosion and the redeposition of the material by sheet-wash (water-lain sedimentation) on slope. Water-lain sedimentation may be responsible for the flow-transverse fabric which appears in laminated sediment (they often contain loess and paleosol laminas as well) in the study of Cérna Valley section (Bradák et al. 2011; Bradák-Hayashi et al. 2016). Such magnetic fabric forming processes may also appear in interglacial/humid and glacial/arid phases in regions with poor vegetation cover and higher precipitation in favourable topographical conditions (i.e. on slope).

### 5.3 Case study from Paks - The use of anisotropy parameters as climate proxies

Along with the orientation of the principal susceptibility axes (i.e., the record of prevailing wind direction), the vertical distribution of anisotropy parameters has been used as climate proxies since the early 2000s. Zhu et al. (2004) identified the magnetic fabric parameters  $L$  and declination of  $\kappa_{\max}$  as sensitive proxies for rapid fluctuations in winter and summer monsoons. Such fluctuations also correlated with the cold and warm events of the marine oxygen isotope record GISP2 and the Dansgaard–Oeschger cycles (e.g., Bond et al. 1999).

Magnetic fabric parameters seem to be sensitive indicators of climatic transitions, such as the mid-Brunhes Event (MBT; Jansen et al. 1986). Significant increases in the fluctuation of  $P$  and  $F$  between glacials and interglacials from approximately 400 ka are thought to indicators of changes in the atmospheric circulation related to MBT (Peng et al. 2015).

A complex pattern of the anisotropy parameters was found during another characteristic transition, namely between the Neogene and Quaternary (Xie et al. 2016). Magnetic fabric parameters behave very similarly during the interglacial periods of the Pleistocene and during the Neogene, which was characterized by humid and warm in East Asia. In general, the glacial periods

were characterized by significantly different AMS parameters compared with interglacials and the Neogene. In addition, a horizon indicated by irregular AMS data clearly demonstrates the transition period between the Neogene and Pleistocene.

#### 5.2.1 The identification of orbital forcing and ice sheet dynamics

In addition to the examples above, the vertical distribution of magnetic fabric parameters has been used in paleoclimate and paleoenvironment reconstruction by e.g., Matasova et al., 2001; Lagroix and Banerjee, 2004; Liu and Sun, 2012; Taylor and Lagroix, 2015; and Song et al. 2018. Such studies (along with the summary about the influence of various processes on the magnetic fabric in Section 4) showed that magnetic fabric parameters can preserve information about the paleoenvironment (change) and may be applied as paleoclimatic proxies.

In the case study presented here, the changing characteristics of sedimentation and pedogenesis were recorded by the  $k_{lf}$ ,  $P_j$ ,  $F_{lf}$ , confidence angle  $\epsilon_{31}$ , and the declination of magnetic lineation ( $\kappa_{max}$ ) of the units of Paks loess from the section dated back to the period between MIS19 and 10 (see Suppl. Mat. 1 and Section 2) to reveal the drivers behind the evolution of the versatile environmental components contributing to sedimentation, and its alteration and represented by the magnetic fabric, the periodicity of the AMS parameters was analysed. Wavelet spectrum analysis was employed using high-resolution AMS data to discover connections between the rhythm of the changing fabric and potential drivers of the change (power spectrum density-psd graphs; Figs. 12 and 13).

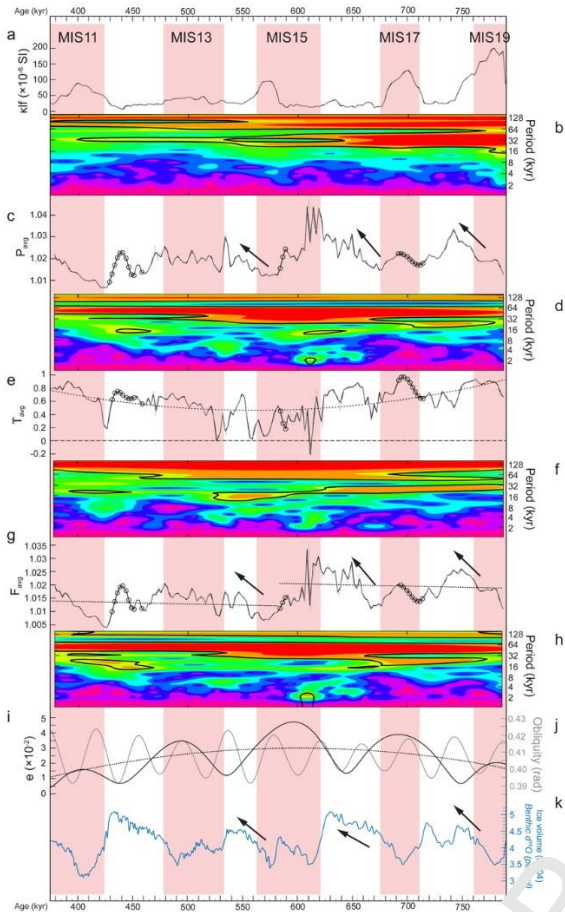


**Figure 12.** Periodicity of magnetic fabric parameters during the early Middle Pleistocene I. Sequences of various magnetic fabric proxies: a) magnetic susceptibility ( $\kappa_{lf}$ ); c) degree of anisotropy ( $P$ ); e) shape of the susceptibility ellipsoid ( $T$ ); and foliation ( $F$ ). The power spectrum density (psd) graphs are b) for  $\kappa_{lf}$ ; d) for  $P$ ; f) for  $T$ ; and h) for  $F$ . The grey curves indicate the original AMS data, and the black curves indicate the resampled series. The black arrows show similar tendencies observed in the rhythms of the AMS parameters and ice volume proxies. The trend lines, e.g., in the sequence of curves e, f and i (in order: shape factor- $T$ , foliation- $F$  and eccentricity- $e$ ), indicate long-term trends in the change in parameters. The colour tones of the psd graphs indicate  $\text{Power}^2$ , i.e., the strength of the identified periodicity in the dataset in order from the strongest to the weakest: red, orange, tones of green (from light to dark), tones of blue (from bright to dark), purple and magenta. Original i) eccentricity; j) obliquity and k) ice volume proxy data were published in Laskar et al. (2011) and Lisiecki and Raymo (2005). See Section 3 and Supplementary Material 1 for

information of data processing, including resampling to compensate for missing data (indicated by circles); wavelet spectrum analysis; and psd graphs.

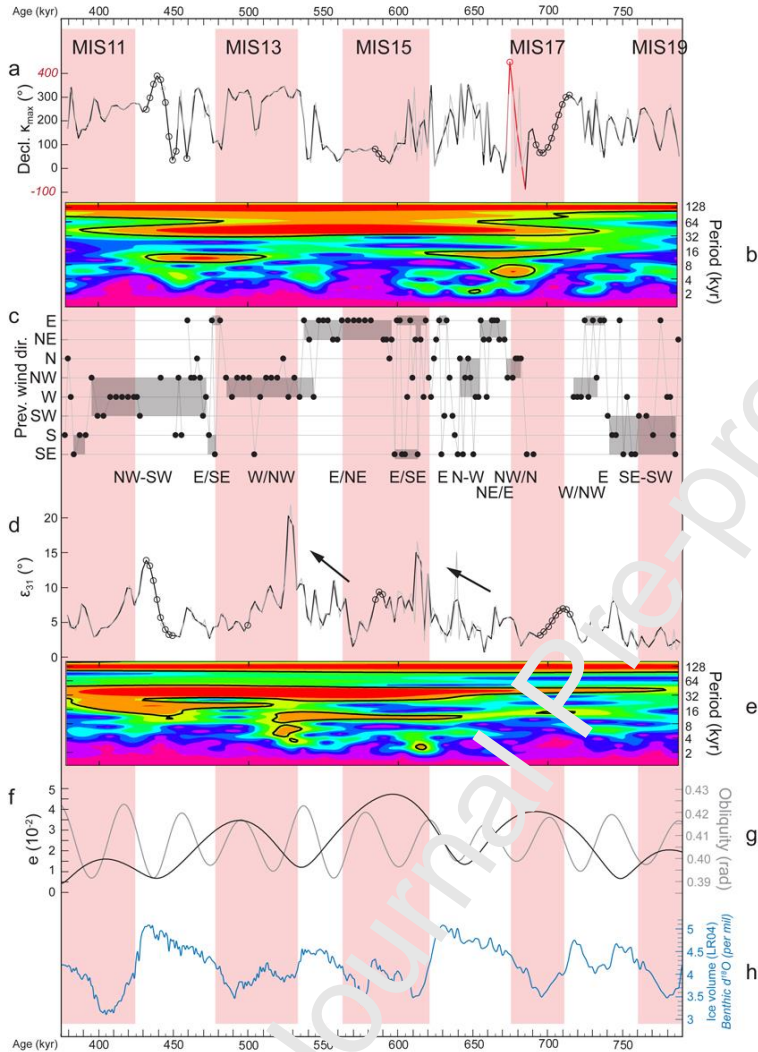


**Figure 13.** Periodicity of magnetic fabric parameters during the early Middle Pleistocene II. Sequences of various magnetic fabric proxies a) declination of magnetic lineation ( $\kappa_{\max}$ ); c) reconstruction of the characteristic paleowind direction; d)  $\epsilon_{31}$  (“foliation plane proxy”). The power spectrum density (psd) graphs are b.) for the declination of  $\kappa_{\max}$  and e.) for  $\epsilon_{31}$ . The grey background colour indicates periods with quasi-permanent prevailing wind direction during the studied period in Fig. 4c. The colour tones of psd graphs indicate Power2, i.e., the strength of the identified periodicity in the dataset in the order from the strongest to the weakest: red, orange, tones of green (from light to dark), tones of blue (from bright to dark) purple and magenta. Original f.) eccentricity (e); g.)

obliquity and h.) ice volume proxy data were published in Laskar et al. (2011) and Lisiecki and Raymo (2005). See Section 3 and Supplementary Material 1, for information on data processing, e.g., resampling to compensate for missing data (indicated by circles); wavelet spectrum analysis; and psd graphs.

The characteristic changes in the AMS proxies were compared with the changes in the orbital parameters, such as obliquity (axial tilt) and eccentricity ( $e$ ) (Figs. 12 and 13), which are known as the most characteristic orbital forcing components of the pre- ( $\epsilon$ ) and post-Early Middle Pleistocene Transition (EMPT) ( $e$ ) paleoclimate (Head and Gibbard, 2005). Characteristic wind directions, which are influenced by growing ice sheets, are demonstrated by the application of the AMS method in European loess profiles (Sub-section 5.1.2; Fig. 10) and suggest similarities between the ice volume proxy (Lisiecki and Raymo, 2005) and the AMS parameters and paleowind direction from the Paks profile (Figs. 12 and 13).

All the studied parameters follow an approximate 100 to 130 kyrs rhythm, which may refer to the periodicity of eccentricity, the predominant orbital forcing component after the amplitude switch during the EMPT (Head and Gibbard, 2005) (Figs. 12 and 13). Although this rhythm appears in every studied parameter, including the change of P and F,  $e$  does not play the most important role. Rather, it is an approximate 40 to 60 kyr periodicity component. This periodicity is most likely connected to obliquity, the pre-EMPT main contributor in orbital forcing. Along with P and F, obliquity-related periodicity also appears in the rhythm of  $\kappa_{lf}$  (MIS 19 to 16), the declination of magnetic lineation ( $\kappa_{max}$ ) (MIS 16 to 12) and  $\epsilon_{31}$  (MIS 16 to 11). The disappearance of the control of obliquity on  $\kappa_{lf}$  (Fig. 12b), i.e., the change in the rhythm of glacials and interglacials, overlaps the period of the EMPT observed in the CLP (Heslop et al. 2002) and the ELB (Basarin et al. 2014).

Among the orbital components, obliquity has a strong influence on ice volume (Ruddiman, 2006), e.g., continental ice sheets. The appearance of the periodicity of obliquity in AMS parameters may suggest a connection between ice sheet dynamics and climatic conditions represented by the

AMS parameters (Figs. 12 and 13). In the case of MIS 18, 16 and 14 glacials (three out of the four studied), AMS parameters, such as P, F and  $\epsilon_{31}$ , follow the rhythm of ice volume dynamics, i.e., a gradual increasing during the glacial with an abrupt decrease during the glacial/interglacial transition (Figs. 12c, g and k and Fig. 13d). The gradual change in the AMS parameters indicates gradual strengthening of dry and cold glacial climate, the depositional environment of loess, and a peak as an indicator of a 'harsh' environment at the end of the glacial. A gradual change in the AMS parameters and the represented environmental change seems to represent a feedback of growing continental ice in the high latitudes in Europe and the extending influence of a high-pressure climate centre (continental ice sheet air mass, CIAM) over the ice sheet towards the lower latitudes (Fig. 10).

The connection between the ice volume dynamics and the sedimentary environment of loess may be indicated by the trends of longer intervals observed in the changes in F. Similar to the ice volume proxy, the period from MIS 19 to 16 shows more characteristic, higher-amplitude peaks compared to the period until MIS 13 after a reduction during MIS 15 (illustrated by trends in Fig. 12g). The relationship between ice sheet dynamics and loess sedimentation has been suggested to occur in the CLP (e.g., Ding et al. 1999) and in the ELB based on various methods (Nawrocki et al. 2006; Moin et al., 2017). One of the methods involves identifying a connection between the quasi-permanent CIAM formed over the extending continental ice sheets in North Europe and the prevailing northerly wind ('blowing' from the ice sheet) in the region at lower latitudes. This relationship has already been proven by paleowind directions (e.g., by AMS) (Fig. 10), but one unanswered question is whether the paleowind direction indicates the influence of the extending European ice sheet in the Paks section.

Although eccentricity and obliquity (~MIS 16 to MIS 11)-driven periodical changes in wind direction are demonstrated by the psd graph, the results are not sufficiently convincing (Fig. 13a, b and c). Due to the chaotic change in the wind, no clear prevailing direction can be separated by the applied plot(s) represented in Figure 13a and c. To determine the most characteristic wind direction in the studied period, the declination of magnetic lineation ( $\kappa_{\max}$ ) was plotted on a return map, a

commonly used method in the case of chaotic systems (Kapitaniak and Bishop, 1999) (Fig. 14). Compared to other parameters given as examples, the distribution of magnetic lineation did not exhibit periodicity, but the alignment of data in the density map derived from the return map indicates a NW to NE prevailing direction of paleowinds (Fig. 14e). The characteristic northward orientation of paleowinds may support the theory about the extending ice sheet and its climatic impact in mid-latitude Europe (Fig. 10).

The evidence presented here may describe long-term early Middle Pleistocene cooling (Bugge et al., 2013) from a new perspective. As a completion and augmentation of the theory presented by Bugge et al. (2013) regarding the effect of Alpine orogenesis (uplift) on climate, we emphasize the influence of continental ice sheets and the EMPT as factors in the progressive evolution of the paleoclimate in East and Central Europe (Bugge et al., 2013; Bradák et al., 2019b). Evidence, such as similarities between the rhythm of ice volume and magnetic fabric parameters and the prevailing wind direction, may verify the influence of a high-pressure climatic centre that formed over the ice sheet. The climatic response to the constant cold air masses of the CIAM might support the long-term transition from a relatively warm (sub-Mediterranean) climate towards colder, continental (Bugge et al., 2013) and North Atlantic air masses (Bradák et al., 2019b) during the early Middle Pleistocene.

As it was demonstrated above, wavelet analysis can be applied with promising results on AMS parameters, but care must be taken during the interpretation of the data. Despite the identified periodicity in some magnetic fabric parameters and the suggested connection of the parameters and climate systems over Europe during the EMPT, the analysis of the AMS are not enough to build a climate model introduced above. The exclusive use of AMS parameters in climate reconstruction may lead to the over-interpretation of the data, therefore more supporting measurements are needed which can verify the existence of such climate model. Various rock and enviromagnetic measurements can provide information about environment related magnetic contributors in the succession and allow the reconstruction of other climate components. Along with paleowind

information, e.g. the reconstruction of paleoprecipitation can provide significant information during building paleoclimate models.

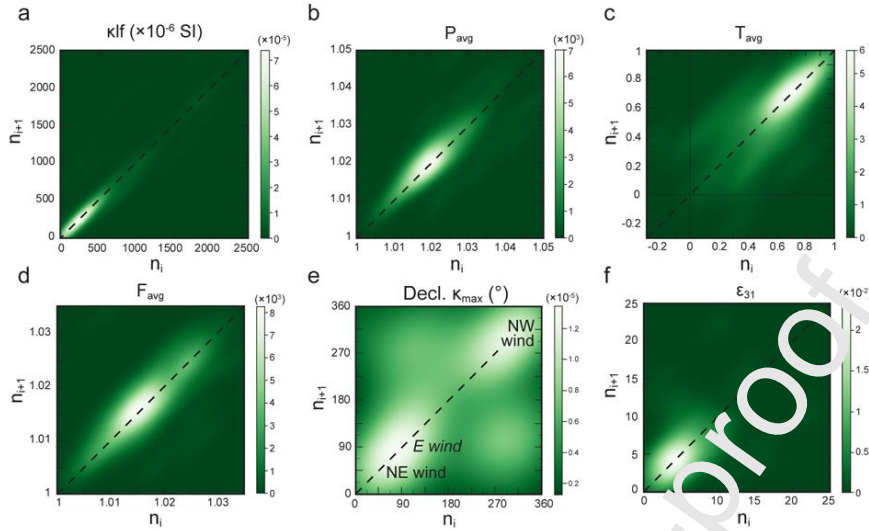


**Figure 14.** The density plot based on the return map of magnetic fabric parameters as a) magnetic susceptibility; b.) degree of anisotropy (P); c.) shape of the susceptibility ellipsoid (T); d.) foliation (F); declination of magnetic lineation ( $\kappa_{max}$ , paleowind direction proxy) and  $\epsilon_{31}$ . The bright areas are the most frequent data in the sequence. The quasi-linear alignment of the most frequent data along an axis from the origin towards the x\_max and y\_max coordinate on the plot (dashed line) suggests stronger periodicity (a, b and d). The chaotic, scattered alignment of the most frequent data of e) shows characteristic values, i.e., indicates NE and NW prevailing wind. See Sub-section 3 for more information about the return map.

## 6. Conclusion

This review summarizes the knowledge about the magnetic fabric of loess derived from approximately thirty studies in the last three decades and introduces the main directions of anisotropy studies, especially but not limited to the determination of prevailing wind direction in

various loess regions during the Quaternary. As summarized below, there are still some “undiscovered areas” in the field of the magnetic fabric research of loess, which represent aims for future investigations.

Studies from, e.g., Hus (2003), Lagroix and Banerjee (2002) and Taylor and Lagroix (2015) suggest the role of paramagnetic contributors in the magnetic fabric of loess. As summarized by Lagroix and Banerjee (2002), paramagnetic silicates (common loess minerals) have oblate AMS ellipsoids (e.g., Borradaile 1988; Borradaile and Werner, 1994; Borradaile and Henry, 1997), and magnetite (one of the most common ferromagnetic contributors) is prolate (e.g., Heider et al. 1987). Oblateness defines the minimum susceptibility, whereas prolateness defines the maximum susceptibility orientation. Therefore, magnetic foliation is defined by paramagnetic silicates and magnetic lineation by ferromagnetic (magnetite) minerals in (Alaskan) loess (Lagroix and Banerjee, 2002). Although the fabric of aeolian loess is strongly foliated, i.e., probably defined by the paramagnetic contributors, no systematic examination has been performed to assess the influence of the paramagnetic minerals during the interpretation of the magnetic fabric of loess.

The main goal of the magnetic fabric research, namely the reconstruction of prevailing wind direction, has outshined other research fields, including the study of the magnetic fabric of paleosols. Studies of various types of paleosols and pedogenic subhorizons via comparisons of various anisotropy methods exhibit potential in future studies and can be used to understand the formation of inverse and vertically oriented magnetic fabrics and the alteration of sedimentary fabric by various pedogenic processes in various pedogenic environments.

Although AMS parameters may work during the separation of various stratigraphical units of individual sections, general rules about the value or behaviour of AMS parameters related to various loess forming geological-pedological processes have not been defined to date. The classification processes suggested by, e.g., Liu et al. (1988) or Bradák and Kovács (2014) may fail if samples from various profiles are investigated. This finding suggests that every loess succession is unique with its own characteristic AMS parameters. Although defining general rules seems almost impossible, the

trend of AMS parameters, as it was shown in the case of Paks succession, can be used for complex paleoclimate and environment reconstruction, which may represent one of the future applications of magnetic anisotropy studies.

Understanding sedimentary and pedogenic processes represented by the behaviour of the magnetic fabric parameters leads their use as climate/environmental proxies. Compared to other enviromagnetic proxies, these proxies may be able to record complex information in addition to simply the prevailing wind direction.

#### Acknowledgements

B. Bradák acknowledges the financial support of project BU2015P18 (Junta de Castilla y Leon, Spain) and the European Regional Development Fund (ERD), project PID2019-108753GB-C21 / AEI / 10.13039/501100011033 of the Agencia Estatal de Investigación and project PID2019-105796GB-100 / AEI / 10.13039/501100011033 of the Agencia Estatal de Investigación. A fellowship was awarded to B. Bradák at Kobe University, Japan, by the Japan Society for the Promotion of Science (JSPS; P15328) during the period of 2015.10 - 2017.10. We are also thankful for the inspiring ideas and comments of our anonymous reviewers.

#### References

- Afifi, A., Clark, V.A., May, S., Raton, B., 2004. Computer-aided Multivariate Analysis, fourth ed. Chapman & Hall/CRC, 489 p.
- Amante, C. Eakins, B.W. 2009. ETOPO1 1 Arc-Minute Global Relief Model: Procedures, Data Sources and Analysis. NOAA Technical Memorandum NESDIS NGDC-24. National Geophysical Data Center, NOAA. doi:10.7289/V5C8276M. <https://data.nodc.noaa.gov/cgi-bin/iso?id=gov.noaa.ngdc.mgg.dem:316>

- Baas, J.H., Hailwood, E.A., McCaffrey, W.D., Kay, M., Jones, R., 2007. Directional petrological characterisation of deep-marine sandstones using grain fabric and permeability anisotropy: methodologies, theory, application and suggestions for integration. *Earth Sci. Rev.* 82, 101–142. <https://doi.org/10.1016/j.earscirev.2007.02.003>
- Balsey, J.R., Buddington, A.F. 1960. Magnetic susceptibility anisotropy and fabric of some Adirondack granites and orthogneisses, *American Journal of Science (Bradley volume)*, 258-A, 6–20.
- Basarin, B., Buggle, B., Hambach, U., Marković, S. B., Dhand, K. O., Kovačević, A., Stevens, T., Guo, Z., Lukić, T., 2014. Time-scale and astronomical forcing of Serbian loess–paleosol sequences: Global and Planetary Change 122, p. 89–106. <https://doi.org/10.1016/j.gloplacha.2014.08.007>
- Batchelor, C.L., Margold, M., Krapp, M., Murton, D.K., Dalton, J. S., Gibbard, P.L., Stokes, C.R., Murton, J.B., Manica, A. 2019. The configuration of Northern Hemisphere ice sheets through the Quaternary. *Nature Communications* (2019) 10:3713, <https://doi.org/10.1038/s41467-019-11601-2> | [www.nature.com/naturecommunications](http://www.nature.com/naturecommunications)
- Begét, J.E. and Hawkins, D.B. 1989. Influence of orbital parameters on Pleistocene loess deposition in central Alaska. *Nature* 337, 151-153. <https://doi.org/10.1038/337151a0>
- Benedetto, J.J., and Frazier, M.W., eds., 1994, *Wavelets: mathematics and applications*: CRC Press, Boca Raton, 592 p. ISBN 9780849382717
- Biedermann, A. R., Koch, C. E., Lorenz W. E. A., Hirt, A. M. 2014. Low-temperature magnetic anisotropy in micas and chlorite. *Tectonophysics* 629, 63–74. <https://doi.org/10.1016/j.tecto.2014.01.015>
- Bilardello, D. 2016. Magnetic anisotropy: theory, instrumentation and techniques. Reference Module in Earth Systems and Environmental Sciences, Elsevier, 2016. 08-Mar-2016 doi: 10.1016/B978-0-12-409548-9.09516-6.
- Bilardello, D., Jackson, M. J. 2014. A comparative study of magnetic anisotropy measurement techniques in relation to rock-magnetic properties. *Tectonophysics* 629, 39–54. <https://doi.org/10.1016/j.tecto.2014.01.026>

- Bond, G.C., Showers, W., Elliot, M., Evans, M., Lotti, R., Hajdas, I., Bonani, G., Johnson, S. 1999. The North Atlantic's 1–2 kyr climate rhythm: relation to Heinrich events, Dansgaard/Oeschger cycles and the little ice age. In Clark, P.U.; Webb, R.S.; Keigwin, L.D. (eds.). *Mechanisms of Global Change at Millennial Time Scales*. Geophysical Monograph. American Geophysical Union, Washington DC. pp. 59–76. ISBN 978-0-87590-033-9.
- Borradaile, G.J. 1988. Magnetic susceptibility, petrofabrics and strain, *Tectonophysics* 156, 1-20. [https://doi.org/10.1016/0040-1951\(88\)90279-X](https://doi.org/10.1016/0040-1951(88)90279-X)
- Borradaile, G.J., Henry, B. 1997. Tectonic applications of magnetic susceptibility and its anisotropy, *Earth Sci. Rev.* 42, 49-93. [https://doi.org/10.1016/S0012-8252\(96\)00044-X](https://doi.org/10.1016/S0012-8252(96)00044-X)
- Borradaile, G.J., Werner, T. 1994. Magnetic anisotropy of some phyllosilicates, *Tectonophysics* 235, 223-248. [https://doi.org/10.1016/0040-1951\(94\)90196-1](https://doi.org/10.1016/0040-1951(94)90196-1)
- Bösken, J., Obreht, I., Zeeden, C., Klasen, N., Hamann, U., Sümegei, P., Lehmkuhl, F. 2019. High-resolution paleoclimatic proxy data from the MIS3/2 transition recorded in northeastern Hungarian loess. *Quaternary International* 502, 95-107. <https://doi.org/10.1016/j.quaint.2017.12.008>
- Bradák B. 2009. Application of anisotropy of magnetic susceptibility (AMS) for the determination of paleo-wind directions during the accumulation period of Bag Tephra, Hungary. *Quaternary International* 198, 77–84. <https://doi.org/10.1016/j.quaint.2007.11.005>
- Bradák, B., Kovács, J., 2013. Quaternary surface processes indicated by the magnetic fabric of undisturbed, reworked and fine-layered loess in Hungary. *Quaternary International* 319, 76–87. <https://doi.org/10.1016/j.quaint.2013.02.009>
- Bradák, B., Thamó-Bozsó, E., Kovács, J., Márton, E., Csillag, G., Horváth, E., 2011. Characteristics of Pleistocene climate cycles identified in Cérna Valley loess–paleosol section (Vértesacsá, Hungary). *Quaternary International*, 234, 86–97. <https://doi.org/10.1016/j.quaint.2010.05.002>
- Bradák, B., Újvári, G., Seto, Y., Hyodo, M., Végh, T. 2018a. A conceptual magnetic fabric development model for the Paks loess in Hungary. *Aeolian Research* 30, 20–31. <https://doi.org/10.1016/j.aeolia.2017.11.002>

- Bradák, B., Seto, Y., Hyodo, M., Szeberényi, J. 2018b. Relevance of ultrafine grains in the magnetic fabric of paleosols. *Geoderma* 330, 125–135.
- Bradák, B., Kovács, J., Magyar, Á. 2019a. The origin and significance of some 'irregular' loess magnetic fabric found in the Paks succession (Hungary). *Geophys. J. Int.* 217, 1742–1754  
<https://doi.org/10.1093/gji/ggz117>
- Bradák, B., Seto, Y., Nawrocki, J. 2019b. Significant pedogenic and palaeoenvironmental changes during the early Middle Pleistocene in Central Europe. *Palaeogeography, Palaeoclimatology, Palaeoecology* 534, 109335. <https://doi.org/10.1016/j.palaeo.2019.109335>
- Bradák, B., Seto, Y., Csonka, D., Végh, T., and Szeberényi, J., 2019c. The hematite-goethite enhancement model of loess and an 'irregular' case from Paks, Hungary. *Journal of Quaternary Science* 34, 299–308. ISSN 0267-8179. <https://doi.org/10.1002/jqs.3101>
- Bradák-Hayashi, B., Biró, T., Horváth, E., Végh, T., Csillag, G. 2016. New aspects of the interpretation of the loess magnetic fabric, Cérna Valley succession, Hungary. *Quaternary Research* 86, 348–358. <https://doi.org/10.1016/j.yqres.2016.07.007>
- Buggle, B., Hambach, U., Kehl, M., Marković, S.B., Zöller, L., Glaser, B., 2013. The progressive evolution of a continental climate in southeast-central European lowlands during the Middle Pleistocene recorded in loess paleosol sequences. *Geology* 41, 771–774. <https://doi.org/10.1130/G34198.1>
- Buggle, B., Hambach, U., Müller, K., Zöller, L., Marković, S.B., Glaser, B., 2014. Iron mineralogical proxies and Quaternary climate change in SE-European loess–paleosol sequences. *Catena* 117, 4–22. <https://doi.org/10.1016/j.catena.2013.06.012>
- Bunn, A., Korpela, M., Biondi, F., Campelo, F., Mérian, P., Qeadan, F., and Zang, C., 2016, dplR: Dendrochronology Program Library in R. R Package Version 1.6.4 (accessed 17.10.16) <http://CRAN.R-project.org/package=dplR>.
- Bunn, A., 2010, Statistical and visual crossdating in R using the dplR library: *Dendrochronologia* 28, p. 251–258, <http://dx.doi.org/10.1016/j.dendro.2009.12.001>

- Cheng, L., Song, Y., Sun, H., Bradák, B., Orozbaev, R., Zong, X., Liu, H. 2019. Pronounced changes in paleo-wind direction and dust sources during MIS3b recorded in the Tacheng loess, northwest China. *Quaternary International*. <https://doi.org/10.1016/j.quaint.2019.05.002> (in press)
- Daubechies, I., 1990, The wavelet transform, time-frequency localization and signal analysis: *IEEE Trans. Inf. Theory* 36, p. 961-1005, <http://dx.doi.org/10.1109/18.57199>.
- Dearing, J. A., Dann, R. J. L., Hay, K., Lees, J. A., Loveland, P. J., Maher, B. A., O'Grady, K., 1996. Frequency-dependent susceptibility measurements of environmental materials, *Geophys. J. Int.*, 124, 228–240. <https://doi.org/10.1111/j.1365-246X.1996.tb06366.x>
- Derbyshire, E., Billard, A., Vliet-Lanoe, B.V., Lautridou, J.-P., Cremaschi, M., 1988. Loess and paleoenvironment some results of a European joint programme of research. *Journal of Quaternary Science* 3, 147-169. <https://doi.org/10.1002/jqs.3390030206>
- Ding, Z.L., Liu, T.S., Rutter, R.W., Yu, Z., Guo, Z., and Z'ou, R., 1995, Ice-volume forcing of East Asian Winter Monsoon variations in the past 80,000 years. *Quaternary Research* 44, 149–159. <https://doi.org/10.1006/qres.1995.1059>
- Ellwood, B.B., 1979. Sample shape and magnetic grain size: two possible controls on the anisotropy of magnetic susceptibility variability in deep sea sediments. *Earth Planet. Sci. Letters*. 43, 309 – 314. [https://doi.org/10.1016/0012-821X\(79\)90216-4](https://doi.org/10.1016/0012-821X(79)90216-4)
- Ellwood, B.B., Ledbetter, M.T. Johnson, D. A. 1979. Sedimentary fabric tool to delineate a high velocity zone within a deep Western Indian Ocean bottom current. *Marine Geology* 33, M51-55. [https://doi.org/10.1016/0025-3227\(79\)90072-0](https://doi.org/10.1016/0025-3227(79)90072-0)
- Ellwood, B.B., 1984. Bioturbation; minimal effects on the magnetic fabric of some natural and experimental sediments. *Earth and Planetary Science Letters* 67, 367–376. [https://doi.org/10.1016/0012-821X\(84\)90175-4](https://doi.org/10.1016/0012-821X(84)90175-4)
- Ellwood, B.B., Howard, J.H., 1981. Magnetic fabric development in an experimentally produced barchan dune. *Journal of Sedimentary Petrology* 51, 97–100. <https://doi.org/10.1306/212F7C16-2B24-11D7-8648000102C1865D>

- Evans, M. E., 2001. Magnetoclimatology of aeolian sediments. *Geophys. J. Int.*, 144, 495-497.  
<https://doi.org/10.1046/j.0956-540X.2000.01317.x>
- Farge, M., 1992, Wavelet transforms and their applications to turbulence: *Ann. Rev. Fluid Mech.* 24, 395-458, <http://dx.doi.org/10.1146/annurev.fl.24.010192.002143>.
- Fitzsimmons, K.E., Marković, S.B., and Hambach, U., 2012. Pleistocene environmental dynamics recorded in the loess of the middle and lower Danube basin. *Quaternary Science Reviews* 41, 104-118. <https://doi.org/10.1016/j.quascirev.2012.03.002>
- Flinn, D., 1962. On folding during three-dimensional progressive deformation. *Quarterly Journal of the Geological Society of London* 118, 385–433.
- Flood, R.D., Kent, D. V., Shor, A.N., Hall, F.R. 1985. The magnetic fabric of surficial deep-sea sediments in HEBBLE Area (Nova Scotian continental shelf). *Marine Geology* 66, 149-167.  
[https://doi.org/10.1016/0025-3227\(85\)90027-1](https://doi.org/10.1016/0025-3227(85)90027-1)
- Forster, T.H., Heller, F., 1997. Magnetic enhancement path in loess sediments from Tajikistan, China and Hungary. *Geophysical Research Letters* 24/1, 17–20. <https://doi.org/10.1029/96GL03751>
- Forster, Th., Evans, M. E., Heller, F. 1994. The frequency dependence of low field susceptibility in loess sediments. *Geophys. Journal International* 118, 636-642. <https://doi.org/10.1111/j.1365-246X.1994.tb03990.x>
- Ge, J., Guo, Z., Zhao, D., Zhong, Y., Wang, T., Yi, L., Deng, C. 2014. Spatial variations in paleowind direction during the last glacial period in north China reconstructed from variations in the anisotropy of magnetic susceptibility of loess deposits. *Tectonophysics* 629, 353–361.  
<https://doi.org/10.1016/j.tecto.2014.07.002>
- Graham, J.V., 1954. Magnetic susceptibility anisotropy, an unexploited petrofabric element. *Bulletin of the Geological Society of America* 65, 1257–1258.
- Granar, L. 1958. Magnetic measurements on Swedish varved sediments. *Arkivfor Geofysik* 3, 1–40.

- Grinsted, A., Moore, J.C., and Jevrejeva, S., 2004, Application of the cross wavelet transform and wavelet coherence to geophysical time series: *Nonlinear Processes Geophys.* 11, p. 561-566, <http://dx.doi.org/10.5194/npg-11-561-2004>.
- Guerrero-Suarez S, Martín-Hernández F: On the reliability of the ams ellipsoid by statistical methods. *Tectonophysics* (2014) 629(C):75-86. <https://doi.org/10.1016/j.tecto.2014.04.010>
- Haase, D., Fink, J., Haase, G., Ruske, R., Pécsi, M., Richter, H., Altermann, M., Jäger, K.-D., 2007. Loess in Europe—its spatial distribution based on a European Loess Map, scale 1:2,500,000. *Quaternary Science Reviews* 26, 1301–1312. <https://doi.org/10.1016/j.quascirev.2007.02.003>
- Head, M. J., Gibbard, P. L., 2005, Early-Middle Pleistocene transitions: an overview and recommendation for the defining boundary: *Geological Society, London, Special Publications* 247, p. 1-18. <http://dx.doi.org/10.1144/GSL.SP.2005.247.01.01>
- Heider, F., Dunlop, D.J., Sugiura, N. 1987. Magnetic properties of hydrothermally recrystallized magnetite crystals, *Science* 236, 1287-1290. DOI: 10.1126/science.236.4806.1287
- Heller, F., Beat, M., Wang, J., Liu, H., Liu, T.S. 1987. Magnetization and sedimentary history of loess in the central Loess Plateau of China, in : T.S. Liu (Ed.), *Aspects of Loess Research*, China Ocean Press, Beijing, 1987, pp. 147-163.
- Heslop, D. 2015. Numerical strategies for magnetic mineral unmixing. *Earth-Science Reviews* 150, 256-284. <https://doi.org/10.1016/j.earscirev.2015.07.007>
- Heslop, D., Dekkers M.J., and Langeresi, C.G. 2002. Timing and structure of the mid-Pleistocene transition: records from the loess deposits of northern China: *Palaeogeography, Palaeoclimatology, Palaeoecology* 185, p. 133-143. [https://doi.org/10.1016/S0031-0182\(02\)00282-1](https://doi.org/10.1016/S0031-0182(02)00282-1)
- Hrouda, F., 1982. Magnetic anisotropy of rock and its application in geology and geophysics. *Geophysical Survey* 5, 37-82. <https://doi.org/10.1007/BF01450244>
- Hrouda, F., 2011. Models of frequency-dependent susceptibility of rocks and soils revisited and broadened, *Geophys. J. Int.*, 187, 1259–1269. <https://doi.org/10.1111/j.1365-246X.2011.05227.x>

- Hrouda, F., M. Ježek, J. 2018. Frequency-dependent AMS of rocks: A tool for the investigation of the fabric of ultrafine magnetic particles. *Tectonophysics* 629, 27–38. <https://doi.org/10.1016/j.tecto.2014.01.040>
- Hrouda, F., Chadima, M. Ježek, J., Kadlec, J. 2018. Anisotropies of in-phase, out-of-phase, and frequency-dependent susceptibilities in three loess/palaeosol profiles in the Czech Republic; methodological implications. *Stud. Geophys. Geod.* 62, 272–290. <https://doi.org/10.1007/s11200-017-0701-y>
- Huang, X.G., Sun, J.M., 2005. Study of the magnetic fabrics in Chinese loess–paleosols since the last interglacial: implication of the paleowind direction (in Chinese with English abstract). *Quat. Sci.* 25, 516–522.
- Hyodo, M., Sano, T., Matsumoto, M., Seto, Y., Bradák, B., Suzuki, K., Fukuda, J-i., Shi, M., Yang, T. 2020. Nanosized authigenic magnetite and hematite particles in mature-paleosol phyllosilicates: New evidence for a magnetic enhancement mechanism in loess sequences of China. *Journal of Geophysical Research: Solid Earth*, 125, e2019JB018705. <https://doi.org/10.1029/2019JB018705>
- Hus, J.J. 2003. The magnetic fabric of some loess/paleosol deposits. *Physics and Chemistry of the Earth* 28, 689–699. [https://doi.org/10.1016/S1474-7065\(03\)00128-1](https://doi.org/10.1016/S1474-7065(03)00128-1)
- Jackson, M. 1991. Anisotropy of magnetic remanence: a brief review of mineralogical sources, physical origins, and geological applications, and comparison with susceptibility anisotropy. *Pure Appl. Geophys.* 136, 1–28. <https://doi.org/10.1007/BF00878885>
- Jansen, J.H.F., Kuijpers, A., Troelstra, S.R., 1986. A Mid-Brunhes climatic event: long-term changes in global atmosphere and ocean circulation. *Science* 232, 619–622. DOI: 10.1126/science.232.4750.619
- Jelinek, V., 1977. The statistical theory of measuring anisotropy of magnetic susceptibility of rocks and its application. *Gefyzika*, Brno, 88 p.
- Jelinek, V. 1981. Characterization of magnetic fabric of rocks. *Tectonophysics* 79, 63–67. [https://doi.org/10.1016/0040-1951\(81\)90110-4](https://doi.org/10.1016/0040-1951(81)90110-4)

- Jordanova, D., Jordanova, N. 1999. Magnetic characteristics of different soil types from Bulgaria. *Studia Geophysica et Geodaetica* 43, 303-318. <https://doi.org/10.1023/A:1023398728538>
- Jordanova, N., Jordanova, D., Karloukovski, V. 1996. Magnetic fabric of Bulgarian loess sediments derived by using various sampling techniques. *Studia Geophysica et Geodetica* 40, 36–49. <https://doi.org/10.1007/BF02295904>
- Kapitaniak, T., Bishop, S. R., 1999. *The illustrated dictionary of nonlinear dynamics and chaos*: John Wiley and Sons, 267 p.
- Kovács, J., Hatvani, I.G., Korponai, J., Székely Kovács, I., 2010, Morlet wavelet and autocorrelation analysis of long-term data series of the Kis-Balaton water protection system (KBWPS): *Ecol. Eng.* 3, p. 1469-1477, <http://dx.doi.org/10.1016/j.ecoleng.2010.06.020>
- Lagroix, F., Banerjee, S. K., 2002. Paleowind direction from the magnetic fabric of loess profile in central Alaska. *Earth and Planetary Science Letters* 195, 99-102. [https://doi.org/10.1016/S0012-821X\(01\)00564-7](https://doi.org/10.1016/S0012-821X(01)00564-7)
- Lagroix, F., Banerjee, S. K., 2004a. The regional and temporal significance of primary aeolian magnetic fabrics preserved in Alaskan loess. *Earth and Planetary Science Letters* 225, 379-395. <https://doi.org/10.1016/j.epsl.2004.07.003>
- Lagroix, F., Banerjee, S. K., 2004b. Cryptic post-depositional reworking in aeolian sediments revealed by the anisotropy of magnetic susceptibility. *Earth and Planetary Science Letters* 224, 453-459. <https://doi.org/10.1016/j.epsl.2004.05.029>
- Laskar, J., Fienga, A., Gastineau, M., Manche, H., 2011. La2010: a new orbital solution for long-term motion of the Earth: *Astronomy & Astrophysics* 532, A89, DOI: 10.1051/0004-6361/201116836 <https://doi.org/10.1051/0004-6361/201116836>
- Ledbetter, M.T., Ellwood, B.B. 1980. Variations in particle alignment and size in sediments of Vema Channel record Antarctic bottom-water velocity change during the last 40,000 years. In: Craddock, C., (E.d.) *Antarctic Geoscience*, pp. 1033-1038.

- Lisiecki, L. E., Raymo, M. E. 2005. A Pliocene-Pleistocene stack of 57 globally distributed benthic  $\delta^{18}\text{O}$  records: *Paleoceanography* 20, PA1003, <https://doi.org/10.1029/2004PA001071>
- Li, Y., Shi, W., Aydin, A., Beroya-Eitner, M.A., Gao, G. 2020. Loess genesis and worldwide distribution. *Earth-Science Reviews* 201, 102947. <https://doi.org/10.1016/j.earscirev.2019.102947>
- Liu, W.M., Sun, J.M. 2012. High-resolution anisotropy of magnetic susceptibility record in the central Chinese Loess Plateau and its paleoenvironment implications. *Science China, Earth Sciences* 55/3, 488–494. doi: 10.1007/s11430-011-4354-3
- Liu, P., Jin, C.S., Zhang, S., Han, J.M., Liu, T.S., 2008. Magnetic fabric of early Quaternary loess–paleosols of Longdan Profile in Gansu Province and the reconstruction of the paleowind directions. *Chin. Sci. Bull.* 53, 1450–1452.
- Liu, T., Ding, Z. 1993. Stepwise coupling of monsoon circulation to global ice volume variations during the late Cenozoic. *Glob. Planet. Change* 7, 119–130. [https://doi.org/10.1016/0921-8181\(93\)90044-O](https://doi.org/10.1016/0921-8181(93)90044-O)
- Liu, T., Ding, Z. 1998. Chinese loess and the paleomonsoon. *Annu. Rev. Earth Planet. Sci.* 26, 111–145. <https://doi.org/10.1146/annurev.earth.26.1.111>
- Liu, T., Ding, Z., Rutter, N. 1999. Comparison of Milankovitch periods between continental loess and deep sea records over the last 2.5 Ma. *Quat. Sci. Rev.* 18, 1205–1212. [https://doi.org/10.1016/S0277-3791\(98\)00110-3](https://doi.org/10.1016/S0277-3791(98)00110-3)
- Liu, X., Xu, T., Liu, T. 1988. The Chinese loess in Xifeng, II. A study of anisotropy of magnetic susceptibility of loess from Xifeng. *Geophysical Journal* 92, 349–353. <https://doi.org/10.1111/j.1365-246X.1988.tb01147.x>
- Liu, Q., Roberts, A.P., Larrasoana, J.C., Banerjee, S.K., Guyodo, Y., Tauxe, L., Oldfield, F. 2012. Environmental magnetism: Principles and applications. *Reviews of Geophysics*, 50, RG4002, Paper number 2012RG000393
- Lyche, T., and Schumaker, L.L., 1973. On the convergence of cubic interpolating splines: Meir A, and Sharma, A., eds., *Spline Functions and Approximation Theory*: Birkhäuser, p. 169–189.

- Maher, B. A. 2011. The magnetic properties of Quaternary aeolian dusts and sediments, and their palaeoclimatic significance. *Aeolian Research* 3, 87–144. <https://doi.org/10.1016/j.aeolia.2011.01.005>
- Maher, B. A. 2016. Palaeoclimatic records of the loess/palaeosol sequences of the Chinese Loess Plateau. *Quaternary Science Reviews* 154, 23-84. <https://doi.org/10.1016/j.quascirev.2016.08.004>
- Maher, B.A., Taylor, R.M. 1988. Formation of ultrafine-grained magnetite in soils. *Nature* 336, 368–370. <https://doi.org/10.1038/336368a0>
- Marković, S.B., Hambach, U., Stevens, T., Kukla, G.J., Heller, F., McCoy, W.D., Oches, E.A., Buggle, B., Zöller, L. 2011. The last million years recorded at the Stari Slankamen (Northern Serbia) loess-palaeosol sequence: revised chronostratigraphy and long-term environmental trends. *Quat. Sci. Rev.* 30, 1142–1154. <https://doi.org/10.1016/j.quascirev.2011.02.004>
- Marković, S.B., Stevens, T., Kukla, G.J., Hambach, U., Fitzsimmons, K.E., Gibbard, P., Buggle, B., Zech, M., Guo, Z., Hao, Q., Wu, H., O'Hara Dhand, K., Smalley, I., Újvári, G., Sümegei, P., Timar-Gabor, A., Veres, D., Sirocko, F., Vasiljević, D.A., Jary, Z., Svensson, A., Jović, V., Lehmkuhl, F., Kovács, J., Svirčev, Z. 2015. Danube loess stratigraphy — Towards a pan-European loess stratigraphic model. *Earth-Science Reviews* 148, 228-258. <https://doi.org/10.1016/j.earscirev.2015.06.005>
- Martín-Hernández, F., Hirt, A. M., 2003. The anisotropy of magnetic susceptibility in biotite, muscovite and chlorite single crystals *Tectonophysics* 367, 13– 28. [https://doi.org/10.1016/S0040-1951\(03\)00127-6](https://doi.org/10.1016/S0040-1951(03)00127-6)
- Martín-Hernández, F., Ferré, E. C. 2007. Separation of paramagnetic and ferrimagnetic anisotropies: A review. *Journal of Geophysical Research, Solid Earth*, 112, 3, B03105. <https://doi.org/10.1029/2006JB004340>
- Matasova, G., Kazansky, A.Y. 2004. Magnetic properties and magnetic fabrics of Pleistocene loess/palaeosol deposits along west-central Siberian transect and their palaeoclimatic implications. *Geological Society, London, Special Publications* 238, 145–173. <https://doi.org/10.1144/GSL.SP.2004.238.01.11>

- Matasova, G., Petrovský, E., Jordanova, N., Zykina, V., Kapička, A. 2001. Magnetic study of Late Pleistocene loess /palaeosol sections from Siberia: palaeoenvironmental implications *Geophysical Journal International* 147, 367–380. <https://doi.org/10.1046/j.0956-540x.2001.01544.x>
- Mathé, P-E., Rochette, P., Vandamme, D., Colin, F. 1997. The origin of magnetic susceptibility and its anisotropy in some weathered profiles. *Phys. Chem. Earth* 22, 183-187. [https://doi.org/10.1016/S0079-1946\(97\)00100-6](https://doi.org/10.1016/S0079-1946(97)00100-6)
- Mathé, P-E., Rochette, P., Vandamme, D., Colin, F. 1999. Volumetric changes in weathered profiles: iso-element mass balance method questioned by magnetic fabric *Earth and Planetary Science Letters* 167, 255–267. [https://doi.org/10.1016/S0012-821X\(99\)00024-2](https://doi.org/10.1016/S0012-821X(99)00024-2)
- Maxbauer, D.P., Feinberg, J.M., Fox, D.L. 2016. Magnetic mineral assemblages in soils and paleosols as the basis for paleoprecipitation proxies: A review of magnetic methods and challenges. *Earth-Science Reviews* 155, 28-48. <https://doi.org/10.1016/j.earscirev.2016.01.014>
- Moine, O., Antoine, P., Hatté, C., Landais, A., Mathieu, J., Prud'homme, C., Rousseau, D.-D., 2017. The impact of Last Glacial climate variability in west-European loess revealed by radiocarbon dating of fossil earthworm granules. *PNAS* 114, (2016) 214. <https://doi.org/10.1073/pnas.1614751114>
- Morlet, J, Arens, G., Fourgeau, E., Gard, D. 1982. Wave propagation and sampling theory; part I, Complex signal and scattering in multi layered media. *Geophysics* 47, 203-221. <https://doi.org/10.1190/1.1441328>
- Mush, D.R. 2007. Loess deposit, origins and properties. In: Elias, S.A. (ed.) *Encyclopedia of Quaternary Science*, ELSEVIER, pp. 1405-1418.
- Nawrocki, J., Polechońska, O., Boguckij, A., Łanczont, M. 2006. Palaeowind directions recorded in the youngest loess in Poland and western Ukraine as derived from anisotropy of magnetic susceptibility measurements. *Boreas* 35, 266–271. <https://doi.org/10.1111/j.1502-3885.2006.tb01156.x>
- Nawrockia, J., Gozhik, P., Łanczont, M., Pańczyk, M., Komar, M., Bogucki, A., Williams, I.S., Czupyt, Z. 2018. Palaeowind directions and sources of detrital material archived in the Roxolany loess section

- (southern Ukraine). *Palaeogeography, Palaeoclimatology, Palaeoecology* 496, 121–135.  
<https://doi.org/10.1016/j.palaeo.2018.01.028>
- Nawrocki, J., Bogucki, A.B., Gozhik, P., Łanczont, M., Pańczyk, M., Standzikowski, K., Komar, M., Rosowiecka, O., Tomeniuk, O. 2019. Fluctuations of the Fennoscandian Ice Sheet recorded in the anisotropy of magnetic susceptibility of periglacial loess from Ukraine. *Boreas*.  
<https://doi.org/10.1111/bor.12400>. ISSN 0300-9483.
- Norūsis, M.J., 1993. SPSS for Windows Professional Statistic Release 6.0, pp. 385, SPSS Inc.
- Obersteinová, T. 2016. Magnetic fabric of selected loess-paleosol sequences in southern Moravia and central Bohemia. Diploma. Charles University, Praha, 2016. 59 p. (with English abstract).
- Parés, J.M. 2015. Sixty years of anisotropy of magnetic susceptibility in deformed sedimentary rocks. *Frontiers in Earth Science* 3: 4. <http://dx.doi.org/10.3389/feart.2015.00004>.
- Peng, S., Ge, J., Li, C., Liu, Z., Qi, L., Tan, Y., Cheng, Y., Deng, C., Qiao, Y. 2015. Pronounced changes in atmospheric circulation and dust source area during the mid-Pleistocene as indicated by the Caotan loess-soil sequence in North China. *Quaternary International* 372, 97–107.  
<https://doi.org/10.1016/j.quaint.2014.09.015>
- Pokorný, J., Pokorný, P., Suza, P., Hrochová, F. 2011. A multi-function kappabridge for high precision measurement of the AMS and the variations of magnetic susceptibility with field, temperature and frequency. In: Petrovský, F. et al. (eds.), *The Earth's Magnetic Interior*, IAGA Special Sopron Book Series 1, 293-301. DOI 10.1007/978-94-007-0323-0\_20,
- Pye, K. 1987. *Aeolian dust and dust deposits*. Academic Press, San Diego, CA, 330p.
- Rees, A. I. 1961. The effect of water currents on the magnetic remanence and anisotropy of susceptibility of some sediments. *Geophys. J. R. Astron. Soc.* 5, 235–251. doi: 10.1111/j.1365-246X.1961.tb00431.x
- Rees, A. I. 1965. The use of anisotropy of magnetic susceptibility in the estimation of sedimentary fabric. *Sedimentology* 4, 257–271. doi: 10.1111/j.1365-3091.1965.tb01550.x

- Rees, A.I., 1966. The effect of depositional slopes on the anisotropy of magnetic susceptibility of laboratory deposited sands. *J. Geol.* 74, 856–867. <https://doi.org/10.1086/627216>
- Rees, A.I., 1968. The production of preferred orientation in a concentrated dispersion of elongated and flattened grains. *J. Geol.* 76, 457–465. <https://www.jstor.org/stable/30064654>
- Rees, A.I., 1983. Experiments on the production of traverse grain alignment in a sheared dispersion. *Sedimentology* 30, 437–448. <https://doi.org/10.1111/j.1365-3091.1983.tb00682.x>
- Rees, A.I., Woodall, W.A., 1975. The magnetic fabric of some laboratory-deposited sediments. *Earth Planet. Sci. Lett.* 25, 121–130. [https://doi.org/10.1016/0012-821X\(75\)90188-0](https://doi.org/10.1016/0012-821X(75)90188-0)
- Rees, A.I., Brown, C.M., Hailwood, E. A., Riddy, P.J. 1982. Magnetic fabric of bioturbated sediment from the Northern Rockall Trough: comparison with modern currents. *Marine Geology* 46, 161-173. [https://doi.org/10.1016/0025-3227\(82\)90157-8](https://doi.org/10.1016/0025-3227(82)90157-8)
- Reinders, J., Hambach, U. 1995. A geomagnetic event recorded in loess deposits of the Tonchesberg (Germany): identification of the Blake magnetic polarity episode. *Geophys. J. Int.* 122, 407-418. <https://doi.org/10.1111/j.1365-246X.1995.tb07604.x>
- Roberts, A. P., Almeida, T. P., Church, N. S., Harrison, R. J., Heslop, D., Li, Y., Li, Y., Muxworthy, A. R., Williams, W., Zhao, X. 2017. Resolution of the origin of pseudo-single domain magnetic behavior. *Journal of Geophysical Research: Solid Earth*, 122, 9534–9558. <https://doi.org/10.1002/2017JB014860>
- Rochette, P. 1988. Inverse magnetic fabric in carbonate-bearing rocks. *Earth and Planetary Science Letters* 90, 229-237. [https://doi.org/10.1016/0012-821X\(88\)90103-3](https://doi.org/10.1016/0012-821X(88)90103-3)
- Rochette, P., Fillion, G. 1988. Identification of multi component anisotropies in rocks using various field and temperature values in a cryogenic magnetometer. *Phys. Earth Planet. Inter.* 51, 379–386. [https://doi.org/10.1016/0031-9201\(88\)90079-9](https://doi.org/10.1016/0031-9201(88)90079-9)
- Rochette, P., Jackson, M., Aubourg, C. 1992. Rock magnetism and the interpretation of anisotropy of magnetic susceptibility, *Rev. Geophys.*, 30(3), 209–226. <https://doi.org/10.1029/92RG00733>
- Ruddiman, W. F., 2006, Orbital changes and climate, *Quaternary Science Reviews* 25, p. 3092–3112. <https://doi.org/10.1016/j.quascirev.2006.09.001>

- Scotese, C.R. 2013. Map Folio 2, Last Glacial Maximum (Pleistocene, 21 ky). PALEOMAP PaleoAtlas for ArcGIS, vol. 1, Cenozoic Paleogeographic, Paleoclimatic and Plate Tectonic Reconstructions, PALEOMAP Project, Evanston, IL.
- Song, Y., Fang, X., King, J. W., Li, J., Naoto, I., An, Z., 2014. Magnetic parameter variations in the Chaona loess/paleosol sequences in the central Chinese Loess Plateau, and their significance for the middle Pleistocene climate transition. *Quaternary Research* 81, 433–444.  
<https://doi.org/10.1016/j.yqres.2013.10.002>
- Song, Y., Guo, Z., Marković, S., Hambach, U., Deng, C., Chang, L., Wu, J., Hao, Q. 2018. Magnetic stratigraphy of the Danube loess: A composite Titel-Stari Slankamen loess section over the last one million years in Vojvodina, Serbia. *Journal of Asian Earth Sciences* 155, 68–80.  
<https://doi.org/10.1016/j.jseaes.2017.11.012>
- Spassov, S., Heller, F., Kretzschmar, R., Evans, M.E., Yue, L.P., Nourgaliev, D.K. 2003. Detrital and pedogenic magnetic mineral phases in the loess/palaeosol sequence at Lingtai (Central Chinese Loess Plateau). *Physics of the Earth and Planetary Interiors* 140, 255–275.  
<https://doi.org/10.1016/j.pepi.2003.05.003>
- Stacey, F.D., Joplin, G., Lindsay, J. 1960. Magnetic anisotropy and fabric of some foliated rock from S.E. Australia. *Geophysica Pura Appl.* 47, 30-40.
- Stockburger, D.W., 2001. *Multivariate Statistics: Concepts, Models, and Applications*. Missouri State University. <http://www.psv.hstat.missouristate.edu/multibook/mlt00.htm>.
- Sun, J. M., Ding, Z. L., Liu, T.S. 1995. Primary application of magnetic susceptibility measurement of loess and paleosols for reconstruction of winter monsoon direction (in Chinese), *Chin. Sci. Bull.* 40, 1976-1978.
- Taira, A., 1989. Magnetic fabrics and depositional processes. In: Taira, A., Masuda, F. (Eds.), *Sedimentary Facies in the Active Plate Margin*. Terra Scientific Publishing Company, Tokyo, pp. 43–77.

- Tarling, D.H., Hrouda, F. 1993. The magnetic anisotropy of rocks, Chapman and Hall, London, Glasgow, New York, Tokyo, Melbourne, Madras, 218.
- Tauxe, L., 2010. Essentials of paleomagnetism. Berkeley: University of California Press, 489 p.
- Tauxe, L., Mullender, T. A. T., Pick, T. 1996. Potbellies, wasp-waists and superparamagnetism in magnetic hysteresis. *Journal of Geophysical Research* 101, 571–583.  
<https://doi.org/10.1029/95JB03041>
- Taylor, S.N., Lacroix, F. 2015. Magnetic anisotropy reveals the depositional and post-depositional history of a loess-paleosol sequence at Nussloch (Germany): AMS of Nussloch loess-paleosol sequence, *Journal of Geophysical Research, Solid Earth*, 120, doi:10.1002.  
<https://doi.org/10.1002/2014JB011803>
- Thistlewood, L., Sun, J.Z., 1991. A palaeomagnetic and mineral magnetic study of the loess sequence at Liujiapo, Xian, China. *J. Quat. Sci.* 6, 13–26. <https://doi.org/10.1002/jqs.3390060104>
- Thamó-Bozsó, E., Kovács, L. Ó., Magyar, Á., Marsi, I. 2014. Tracing the origin of loess in Hungary with the help of heavy mineral composition data. *Quaternary International* 319, 11–21.  
<https://doi.org/10.1016/j.quaint.2013.04.003>
- Újvári, G., Varga, A., Ramos, F. C., Kovács, J., Németh, T., Stevens, T. 2012. Evaluating the use of clay mineralogy, Sr–Nd isotopes and zircon U–Pb ages in tracking dust provenance: An example from loess of the Carpathian Basin. *Chemical Geology*, 304–305, 83–96.  
<https://doi.org/10.1016/j.chemgeo.2012.02.007>
- Újvári G, Varga A, Raucsik B, Kovács J. 2014. The Paks loess-paleosol sequence: a record of chemical weathering and provenance for the last 800 ka in the mid-Carpathian Basin. *Quaternary International* 319, 22-37. <https://doi.org/10.1016/j.quaint.2012.04.004>
- Xie, X., Xian, F., Wu, Z., Kong, X., Chang, Q., 2016. Asian Monsoon variation over the late Neogene–early Quaternary recorded by Anisotropy of Magnetic Susceptibility (AMS) from Chinese loess. *Quaternary International* 399, 183-189. <https://doi.org/10.1016/j.quaint.2015.04.061>

- Yang, T., Hyodo, M., Zhang, S., Maeda, Yang, Z., Wu, H. & Li, H., 2013. New insights into magnetic enhancement mechanism in Chinese paleosols, *Palaeogeography, Palaeoclimatology, Palaeoecology*, 369, 493–500. <https://doi.org/10.1016/j.palaeo.2012.11.016>
- Varga, Gy., Cserhádi, Cs., Kovács, J., Szalai, Z. 2016. Saharan dust deposition in the Carpathian Basin and its possible effects on interglacial soil formation. *Aeolian Research* 22, 1–12. <https://doi.org/10.1016/j.aeolia.2016.05.004>
- Vidakovic, B., 2009, *Statistical Modeling by Wavelets*: John Wiley & Sons, New Jersey, 408 p.
- von Rad, U. 1970. Comparison between "magnetic" and sedimentary fabric in graded and cross-laminated sand layers, Southern California. *Geol. Rundsch.* 60, 321–354.
- Wang, R, Løvlie, R. 2010. Subaerial and subaqueous deposition of loess: Experimental assessment of detrital remanent magnetization in Chinese loess. *Earth and Planetary Science Letters* 298, 394–404. <https://doi.org/10.1016/j.epsl.2010.08.019>
- Wang, J.L., Fang, X.M., Zhang, Y.T., Cao, J.X., 1995. The anisotropy of loess magnetic susceptibility in the northeastern fringe of Qinghai–Xizang (Tibetan) Plateau as an indicator of paleowind direction. *J. Lanzhou Univ. (Nat. Sci. Ed.)* 31, 155–159
- Wells, M.A., Fitzpatrick, R.W., Gilkes, P.J., Dobson, J. 1999. Magnetic properties of metal-substituted haematite. *Geophysical Journal International* 138/2, 571–580. <https://doi.org/10.1046/j.1365-246X.1999.00840.x>
- Zan, J., Fang, X., Kang, J., Li, X., Yan, M. 2020. Spatial and altitudinal variations in the magnetic properties of eolian deposits in the northern Tibetan Plateau and its adjacent regions: Implications for delineating the climatic boundary. *Earth-Science Reviews* 208, 103271. <https://doi.org/10.1016/j.earscirev.2020.103271>
- Zeeden, C., Hambach, U., Händel, M., 2015. Loess magnetic fabric of the Krems-Wachtberg archaeological site. *Quatern. Int.* 372, 188–194. <https://doi.org/10.1016/j.quaint.2014.11.001>
- Zhang, R., Kravchinsky, V. A., Zhu, R., Leping, Y., 2010. Paleomonsoon route reconstruction along a W-E transect in the Chinese Loess Plateau using the anisotropy of magnetic susceptibility: Summer

monsoon model. Earth and Planetary Science Letters 299, 436-446.

<https://doi.org/10.1016/j.epsl.2010.09.026>

Zhong, W., Fang, X.M., Cao, J.X., Wang, J.L., 1996. Study on the magnetic fabric features of the samples taken from Dongshanding profile in Linxia Basin, Gansu Province. J. Lanzhou Univ. (Nat. Sci.) 32, 116–120.

Zhu, R., Liu, Q., Jackson, M.J. 2004. Paleoenvironmental significance of the magnetic fabric of Chinese loess-paleosols since the last interglacial (< 130 ka). Earth and Planetary Science Letters 221, 55–69.  
[https://doi.org/10.1016/S0012-821X\(04\)00103-7](https://doi.org/10.1016/S0012-821X(04)00103-7)

Supplementary Material 1. The collection of anisotropy of low field magnetic susceptibility data, the calculated age model and the dataset used during the wavelet analysis.

- Decades of loess magnetic fabric study is summarized.
- New results about the influence of pedogenesis in magnetic fabric are presented.
- Role of magnetic fabric studies in regional-continental level climate reconstruction are revealed.
- Potential future key topics in loess magnetic fabric research are appointed.

Journal Pre-proof

June 2020

Editorial Board

*Earth-Science Reviews*

Dear Alessandra Negri and Timothy James Horscroft

As corresponding author, I am submitting a manuscript to you for *Earth-Science Reviews*. The title is "***Magnetic fabric of loess and its significance in Pleistocene environment reconstructions***" by Balázs Bradák, Yusuke Seto, Martin Chadima, József Kovács, Péter Tanos, Gábor Újvári, Masayuki Hyodo declare that there is no conflict of interest.